Developing and analyzing an explicit unconditionally stable finite element scheme for an equivalent Bérenger's PML model *

Yunqing Huang † Jichun Li ‡ Xin Liu §

October 5, 2022

Abstract

The original Bérenger's perfectly matched layer (PML) was quite effective in simulating wave propagation problem in unbounded domains. But its stability is very challenging to prove. Later, some equivalent PML models were developed by Bécache and Joly [4] and their stabilities were established. Hence studying and developing efficicent numerical methods for solving those equivalent PML models are needed and interesting. Here we propose a novel explicit unconditionally stable finite element scheme to solve an equivalent Bérenger's PML model. Both the stability and convergence analysis are proved for the proposed scheme. Numerical results justifying the theoretical analysis are presented. We also demonstrate the effectiveness of this PML in simulating wave propagation in the free space. To our best knowledge, this is the first explicit unconditionally stable finite element scheme developed for this PML model.
Keywords − Maxwell's equations, Perfectly Matched Layer, finite element method.
Mathematics Subject Classification (2000): 65N30, 35L15, 78-08

1 Introduction

In 1994, Bérenger [7] introduced the perfectly matched layer (PML) techqniue to develop efficient numerical absorbing boundary conditions for solving the time-dependent Maxwell's equations in unbounded domains. This PML technique has been shown to be very effective and can absorb all impinging waves over a wide frequency range. Since 1994, many different PML models have been developed and applied to solve Maxwell's equations in both time-domain [1, 11, 21, 25, 26, 15, 32] and frequency domain [3, 9, 16]. More details and references can be found in the classic computational electromagnetic book [30], a review paper on PMLs [31], and our recent book on metamaterials [22, Ch.8]. Furthermore, the PML technique has been extended to solve other wave propagation problems in different media, such as acoustics, elastodynamics [2, 14], elasticity [20], anisotropic dispersive media [6] and metamaterials [12, 13, 5]. Due to many potential applications of metamaterials such as design of invisibility cloaks, recently there has been a growing interest in the study of the Maxwell's equations involving metamaterials (e.g., [8, 23, 24, 33]).

Even though the original splitted Bérenger PML works very well in practical numerical simulations, the mathematical analysis of its energy stability for the general variable damping function case is still an open problem. Until 2002, Bécache and Joly [4] managed to establish a stability result for an equivalent Bérenger PML model. Inspired by their work, recently we [19, 17] proposed and analyzed some finite diffence and finite element methods for solving those equivalent PML models. Those schemes we proposed so far are explicit and has a time step constraint. In 2021, we [18] discovered a novel technique in constructing an explicit unconditionally finite element method for solving Maxwell's equations in the free space and in Drude metamaterials. One major contribution of this paper is that we successfully extend that technique to construct and prove an explicit unconditionally

*This work was partially supported by NSFC project 11971410 and NSF grant DMS-2011943.
†Hunan Key Laboratory for Computation and Simulation in Science and Engineering, Xiangtan University, Xiangtan, China (huangyq@xtu.edu.cn).
‡Department of Mathematical Sciences, University of Nevada Las Vegas, Las Vegas, Nevada 89154-4020, USA (jichun.li@unlv.edu).
§Hunan Key Laboratory for Computation and Simulation in Science and Engineering, Xiangtan University, Xiangtan, China. (xincherry05@163.com).

This provisional PDF is the accepted version. The article should be cited as: ESAIM: M2AN, doi: 10.1051/m2an/2022086

stable scheme for solving this complicated equivalent Bérenger's PML model. This new scheme is not only easy in implementation but also very efficient like other explicit leapfrog type schemes. To the best of our knowledge, this is the first explicit unconditionally stable finite element scheme constructed and analyzed for this PML model.

The rest of the paper is organized as follows. In Sect. 2, we first present the PML model equations and construct a semi-discrete scheme for the PML model. This semi-discrete scheme is a small perturbation of the usual leapfrog scheme for this PML model. This small pertubation plays the magic for the construction of an explicit unconditionally stable scheme. In Sect.3, we first develop our fully-discrete finite element scheme. Then we prove the unconditional stability and the optimal error estimate for this scheme. In Sect. 4, we present some numerical results to confirm our theoretical analysis and further apply our scheme to simulate some practical wave propagation problem to show the long stability of the scheme and the effective wave absorbing property of this equivalent PML model. We conclude the paper in Sect. 5.

2 The model equations and construction of a semi-discrete scheme

By following the idea of [4], we derived the governing equations of an equivalent Bérenger's PML model for the Transverse Electric (TEz) mode given as follows [19, Eqs.(32)-(36)]: for any $(\boldsymbol{x},t)\in\Omega\times(0,T]$,

$$\varepsilon_0\partial_t\boldsymbol{E}+\Sigma^{**}\boldsymbol{E}=\nabla\times H:=(\partial_y H,-\partial_x H)', \tag{1a}$$

$$\varepsilon_0\partial_t\widetilde{\boldsymbol{E}}=\varepsilon_0\partial_t\boldsymbol{E}+\Sigma_{**}\boldsymbol{E}, \tag{1b}$$

$$\mu_0\partial_t H^*=-\nabla\times\widetilde{\boldsymbol{E}}:=-(\partial_x\tilde{E}_y-\partial_y\tilde{E}_x), \tag{1c}$$

$$\partial_t\widetilde{H}=H, \tag{1d}$$

$$\partial_t H+\varepsilon_0^{-1}(\sigma_x+\sigma_y)H+\varepsilon_0^{-2}\sigma_x\sigma_y\widetilde{H}=\partial_t H^*, \tag{1e}$$

where ε_0 and μ_0 are the permittivity and permeability in free space, $\boldsymbol{E}=(E_x,E_y)'$ and H are the electric field and magnetic field, $\widetilde{\boldsymbol{E}}=(\widetilde{E}_x,\widetilde{E}_y)'$, $\widetilde{H}$ and H^* are auxiliary variables, and

$$\Sigma^{**}=diag(\sigma_y,\sigma_x),\ \Sigma_{**}=diag(\sigma_x,\sigma_y).$$

Moreover $\sigma_x(x),\sigma_y(y)$ are nonnegative damping functions in the x,y directions, respectively. Here, we assume that Ω is an open bounded Lipschitz polygon in $\mathcal{R}^2$ with boundary $\partial\Omega$ and outward unit normal vector $\boldsymbol{n}$. To complete the model problem (1a)-(1e), we further assume that it satisfies the perfect electric conductive (PEC) boundary condition:

$$\boldsymbol{n}\times\boldsymbol{E}=0\quad\text{on}\quad\partial\Omega, \tag{2}$$

and the initial conditions:

$$\boldsymbol{E}(\boldsymbol{x},0)=\boldsymbol{E}_0(\boldsymbol{x}),\quad \widetilde{\boldsymbol{E}}(\boldsymbol{x},0)=\widetilde{\boldsymbol{E}}_0(\boldsymbol{x}),\quad H(\boldsymbol{x},0)=H_0(\boldsymbol{x}),\quad H^*(\boldsymbol{x},0)=H_0^*(\boldsymbol{x}),\quad \widetilde{H}(\boldsymbol{x},0)=\widetilde{H}_0(\boldsymbol{x}),\quad \forall\ \boldsymbol{x}\in\Omega, \tag{3}$$

where $\boldsymbol{E}_0,\widetilde{\boldsymbol{E}}_0,H_0,H_0^*$ and $\widetilde{H}_0$ are some given functions.

First, let us partition the time interval $[0,T]$ uniformly by points $t_i=i\tau, i=0,\cdots,N_t$, where $\tau=\frac{T}{N_t}$ denotes the time step size. Denote $\boldsymbol{E}^n:=\boldsymbol{E}(\cdot,t_n)$. Similar notations are used for other unknowns. Before we derive an explicit unconditionally stable scheme, we first consider a two step scheme of (1a)-(1e):

Step 1:

$$\varepsilon_0\boldsymbol{E}^{n+\frac{3}{2}} = \varepsilon_0\boldsymbol{E}^{n+1}-\frac{\tau}{2}\Sigma^{**}\boldsymbol{E}^{n+1}+\frac{\tau}{2}\nabla\times H^{n+1} \tag{4}$$

$$\varepsilon_0\widetilde{\boldsymbol{E}}^{n+\frac{3}{2}} = \varepsilon_0\widetilde{\boldsymbol{E}}^{n+1}+\varepsilon_0\left(\boldsymbol{E}^{n+\frac{3}{2}}-\boldsymbol{E}^{n+1}\right)+\frac{\tau}{2}\Sigma_{**}\boldsymbol{E}^{n+1} \tag{5}$$

$$\mu_0 H^{*,n+\frac{3}{2}} = \mu_0 H^{*,n+1}-\frac{\tau}{2}\nabla\times\widetilde{\boldsymbol{E}}^{n+1} \tag{6}$$

$$\widetilde{H}^{n+\frac{3}{2}} = \widetilde{H}^{n+1}+\frac{\tau}{2}H^{n+\frac{3}{2}} \tag{7}$$

$$H^{n+\frac{3}{2}} = H^{n+1}-\frac{\tau}{2}\varepsilon_0^{-1}(\sigma_x+\sigma_y)H^{n+\frac{3}{2}}-\frac{\tau}{2}\varepsilon_0^{-2}\sigma_x\sigma_y\widetilde{H}^{n+\frac{3}{2}}+(H^{*,n+\frac{3}{2}}-H^{*,n+1}) \tag{8}$$

Step 2:

$$
\begin{aligned}
\varepsilon_0 \boldsymbol{E}^{n+1} &= \varepsilon_0 \boldsymbol{E}^{n+\frac{1}{2}} - \frac{\tau}{2}\Sigma^{**}\boldsymbol{E}^{n+1} + \frac{\tau}{2}\nabla\times H^{n+1} &(9)\\
\varepsilon_0 \widetilde{\boldsymbol{E}}^{n+1} &= \varepsilon_0 \widetilde{\boldsymbol{E}}^{n+\frac{1}{2}} + \varepsilon_0\left(\boldsymbol{E}^{n+1} - \boldsymbol{E}^{n+\frac{1}{2}}\right) + \frac{\tau}{2}\Sigma_{**}\boldsymbol{E}^{n+1} &(10)\\
\mu_0 H^{*,n+1} &= \mu_0 H^{*,n+\frac{1}{2}} - \frac{\tau}{2}\nabla\times\widetilde{\boldsymbol{E}}^{n+1} &(11)\\
\widetilde{H}^{n+1} &= \widetilde{H}^{n+\frac{1}{2}} + \frac{\tau}{2}H^{n+\frac{1}{2}} &(12)\\
H^{n+1} &= H^{n+\frac{1}{2}} - \frac{\tau}{2}\varepsilon_0^{-1}(\sigma_x+\sigma_y)H^{n+\frac{1}{2}} - \frac{\tau}{2}\varepsilon_0^{-2}\sigma_x\sigma_y\widetilde{H}^{n+\frac{1}{2}} + (H^{*,n+1} - H^{*,n+\frac{1}{2}}) &(13)
\end{aligned}
$$

Reducing all $n's$ in (4) by 1, adding the result with (9), and denoting $\overline{\boldsymbol{E}}^{n+\frac{1}{2}} := \frac{\boldsymbol{E}^{n+1}+\boldsymbol{E}^n}{2}$, we have

$$\varepsilon_0 \boldsymbol{E}^{n+1} = \varepsilon_0 \boldsymbol{E}^n - \tau\Sigma^{**}\overline{\boldsymbol{E}}^{n+\frac{1}{2}} + \frac{\tau}{2}\nabla\times(H^n + H^{n+1}). \quad (14)$$

Reducing all $n's$ in (6) and (8) by 1, and subtracting the result from (11) and (13), respectively, we have

$$\mu_0(H^{*,n+1} + H^{*,n} - 2H^{*,n+\frac{1}{2}}) = -\frac{\tau}{2}\nabla\times\left(\widetilde{\boldsymbol{E}}^{n+1} - \widetilde{\boldsymbol{E}}^n\right), \quad (15)$$

and

$$H^{n+1} + H^n - 2H^{n+\frac{1}{2}} = H^{*,n+1} + H^{*,n} - 2H^{*,n+\frac{1}{2}}. \quad (16)$$

Then substituting (15) and (16) into (14), we have

$$\varepsilon_0 \boldsymbol{E}^{n+1} = \varepsilon_0 \boldsymbol{E}^n - \tau\Sigma^{**}\overline{\boldsymbol{E}}^{n+\frac{1}{2}} + \frac{\tau}{2}\nabla\times\left(2H^{n+\frac{1}{2}} - \frac{\tau}{2\mu_0}\nabla\times(\widetilde{\boldsymbol{E}}^{n+1} - \widetilde{\boldsymbol{E}}^n)\right). \quad (17)$$

Reducing all $n's$ of (5) by 1, and adding the result with (10), we obtain

$$\varepsilon_0 \widetilde{\boldsymbol{E}}^{n+1} = \varepsilon_0 \widetilde{\boldsymbol{E}}^n + \varepsilon_0\left(\boldsymbol{E}^{n+1} - \boldsymbol{E}^n\right) + \tau\Sigma_{**}\overline{\boldsymbol{E}}^{n+\frac{1}{2}}. \quad (18)$$

Adding (6) and (11) together, adding (7) and (12) together, and adding (8) and (13) together, we have

$$
\begin{aligned}
\mu_0 H^{*,n+\frac{3}{2}} &= \mu_0 H^{*,n+\frac{1}{2}} - \tau\nabla\times\widetilde{\boldsymbol{E}}^{n+1}, &(19)\\
\widetilde{H}^{n+\frac{3}{2}} - \widetilde{H}^{n+\frac{1}{2}} &= \tfrac{\tau}{2}(H^{n+\frac{3}{2}} + H^{n+\frac{1}{2}}), &(20)
\end{aligned}
$$

and

$$H^{n+\frac{3}{2}} = H^{n+\frac{1}{2}} - \frac{\tau}{2}\varepsilon_0^{-1}(\sigma_x+\sigma_y)(H^{n+\frac{3}{2}} + H^{n+\frac{1}{2}}) - \frac{\tau}{2}\varepsilon_0^{-2}\sigma_x\sigma_y(\widetilde{H}^{n+\frac{3}{2}} + \widetilde{H}^{n+\frac{1}{2}}) + (H^{*,n+\frac{3}{2}} - H^{*,n+\frac{1}{2}}). \quad (21)$$

Using the following average operator and central difference operator in time:

$$\overline{u}^{n+1} = \frac{1}{2}(u^{n+\frac{3}{2}} + u^{n+\frac{1}{2}}), \quad \delta_\tau u^{n+1} = \frac{1}{\tau}(u^{n+\frac{3}{2}} - u^{n+\frac{1}{2}}),$$

we can be rewrite (17)-(21) as follows:

$$
\begin{aligned}
&\varepsilon_0\delta_\tau \boldsymbol{E}^{n+\frac{1}{2}} + \Sigma^{**}\overline{\boldsymbol{E}}^{n+\frac{1}{2}} = \nabla\times H^{n+\frac{1}{2}} - \frac{\tau^2}{4\mu_0}\nabla\times\nabla\times\delta_\tau\widetilde{\boldsymbol{E}}^{n+\frac{1}{2}}, &(22a)\\
&\varepsilon_0\delta_\tau\widetilde{\boldsymbol{E}}^{n+\frac{1}{2}} = \varepsilon_0\delta_\tau\boldsymbol{E}^{n+\frac{1}{2}} + \Sigma_{**}\overline{\boldsymbol{E}}^{n+\frac{1}{2}}, &(22b)\\
&\mu_0\delta_\tau H^{*n+1} = -\nabla\times\widetilde{\boldsymbol{E}}^{n+1}, &(22c)\\
&\delta_\tau\widetilde{H}^{n+1} = \overline{H}^{n+1}, &(22d)\\
&\delta_\tau H^{n+1} + \varepsilon_0^{-1}(\sigma_x+\sigma_y)\overline{H}^{n+1} + \varepsilon_0^{-2}\sigma_x\sigma_y\overline{\widetilde{H}}^{n+1} = \delta_\tau H^{*,n+1}. &(22e)
\end{aligned}
$$

Remark 1 *It is interesting to remark that the semi-discrete scheme* (22a)-(22e) *can be seen as a small perturbation of a standard explicit leapfrog scheme for solving* (1a)-(1e) *with the first equation added by the last* $O(\tau^2)$ *term. With this extra term, we can develop and prove an explicit unconditionally stable scheme out of* (22a)-(22e) *in the next section.*

3 The fully discrete scheme and its analysis

To solve the problem (1a)-(1e) by a finite element method, we partition the physical domain Ω by a family of regular triangular mesh T_h with maximum mesh size h, and adopt the l-th ($l \geq 1$) order Raviart-Thomas-Nédélec (RTN) mixed finite element spaces $\boldsymbol{V}_h$ and $\boldsymbol{U}_h$ [29, 28, 27]: For any $l \geq 1$,

$$\begin{aligned}
\boldsymbol{V}_h &= \{v_h \in L^2(\Omega): \ v_h|_K \in p_{l-1}, \ \ \forall\ K \in T_h\}, \\
\boldsymbol{U}_h &= \{\boldsymbol{u}_h \in H(\text{curl};\Omega): \ \boldsymbol{u}_h|_K \in (p_{l-1})^2 \oplus S_l, \ \ \forall\ K \in T_h\}, \quad S_l = \{\vec{p} \in (\tilde{p}_l)^2, \boldsymbol{x}\cdot\vec{p} = 0\},
\end{aligned}$$

where $\tilde{p}_l$ denotes the space of homogeneous polynomials of degree l, and p_l denotes the space of polynomials of degree less than or equal to l in variables x, y, respectively. To impose the PEC boundary condition (2), we denote the subspace $\boldsymbol{U}_h^0 = \{\boldsymbol{u} \in \boldsymbol{U}_h : \boldsymbol{u} \times \boldsymbol{n} = 0 \ \text{ on } \partial\Omega\}$.

Now we construct the following leapfrog type scheme for (1a)-(1e): given initial approximations $\boldsymbol{E}_h^0, \widetilde{\boldsymbol{E}}_h^0, H_h^{\frac{1}{2}}, H_h^{*\frac{1}{2}}, \tilde{H}_h^{\frac{1}{2}}$, for any $n \geq 0$, find $\boldsymbol{E}_h^{n+1}, \widetilde{\boldsymbol{E}}_h^{n+1} \in \boldsymbol{U}_h^0$, $H_h^{n+\frac{3}{2}}, H_h^{*n+\frac{3}{2}}, \widetilde{H}_h^{n+\frac{3}{2}} \in \boldsymbol{V}_h$ such that

$$\begin{aligned}
&\varepsilon_0\left(\delta_\tau \boldsymbol{E}_h^{n+\frac{1}{2}}, \boldsymbol{\phi_h}\right) + \left(\Sigma^{**}\overline{\boldsymbol{E}}_h^{n+\frac{1}{2}}, \boldsymbol{\phi_h}\right) = \left(H_h^{n+\frac{1}{2}}, \nabla\times\boldsymbol{\phi_h}\right) \\
&\qquad\qquad - \frac{\tau^2}{4\mu_0}\left(\nabla\times\delta_\tau\widetilde{\boldsymbol{E}}_h^{n+\frac{1}{2}}, \nabla\times\boldsymbol{\phi_h}\right), \qquad \forall \boldsymbol{\phi_h} \in \boldsymbol{U}_h^0, &&\text{(23a)}\\
&\varepsilon_0\left(\delta_\tau \widetilde{\boldsymbol{E}}_h^{n+\frac{1}{2}}, \widetilde{\boldsymbol{\phi}}_h\right) = \varepsilon_0\left(\delta_\tau \boldsymbol{E}_h^{n+\frac{1}{2}}, \widetilde{\boldsymbol{\phi}}_h\right) + \left(\Sigma_{**}\overline{\boldsymbol{E}}_h^{n+\frac{1}{2}}, \widetilde{\boldsymbol{\phi}}_h\right), \qquad \forall \widetilde{\boldsymbol{\phi}}_h \in \boldsymbol{U}_h^0, &&\text{(23b)}\\
&\mu_0\left(\delta_\tau H_h^{*n+1}, \psi_h\right) = -\left(\nabla\times\widetilde{\boldsymbol{E}}_h^{n+1}, \psi_h\right), \qquad \forall \psi_h \in \boldsymbol{V}_h, &&\text{(23c)}\\
&\left(\delta_\tau \widetilde{H}_h^{n+1}, \sigma_x\sigma_y\widetilde{\psi}_h\right) = \left(\overline{H}_h^{n+1}, \sigma_x\sigma_y\widetilde{\psi}_h\right), \qquad \forall \widetilde{\psi}_h \in \boldsymbol{V}_h, &&\text{(23d)}\\
&\left(\delta_\tau H_h^{n+1}, \widehat{\psi}_h\right) + \varepsilon_0^{-1}\left((\sigma_x+\sigma_y)\overline{H}_h^{n+1}, \widehat{\psi}_h\right) + \varepsilon_0^{-2}\left(\sigma_x\sigma_y\overline{\widetilde{H}}_h^{n+1}, \widehat{\psi}_h\right) \\
&\qquad\qquad = \left(\delta_\tau H_h^{*n+1}, \widehat{\psi}_h\right), \qquad \forall \widehat{\psi}_h \in \boldsymbol{V}_h. &&\text{(23e)}
\end{aligned}$$

Note that for theoretical analysis purpose, we multiplied $\sigma_x\sigma_y$ to both sides of (23d).

The initial approximations $\boldsymbol{E}_h^0, \widetilde{\boldsymbol{E}}_h^0$ can be simply obtained by the Nédélec interpolation, while $H_h^{\frac{1}{2}}, H_h^{*\frac{1}{2}}, \tilde{H}_h^{\frac{1}{2}}$ and be done by a Taylor expansion followed by a standard L^2 projections. More specifically, we have the following approximations:

$$\boldsymbol{E}_h^0(\boldsymbol{x}) = \Pi_c\boldsymbol{E}_0(\boldsymbol{x}), \quad \widetilde{\boldsymbol{E}}_h^0(\boldsymbol{x}) = \Pi_c\widetilde{\boldsymbol{E}}_0(\boldsymbol{x}), \tag{24a}$$

$$H_h^{\frac{1}{2}}(\boldsymbol{x}) = P_h\left(H_0(\boldsymbol{x}) + \frac{\tau}{2}\partial_t H(\boldsymbol{x})\right) = P_h\left[H_0 - \frac{\tau}{2}\left(\mu_0^{-1}\nabla\times\widetilde{\boldsymbol{E}}_0 + \varepsilon_0^{-1}(\sigma_x+\sigma_y)H_0 + \varepsilon_0^{-2}\sigma_x\sigma_y\widetilde{H}_0\right)\right], \tag{24b}$$

$$H_h^{*,\frac{1}{2}}(\boldsymbol{x}) = P_h\left(H_0^*(\boldsymbol{x}) + \frac{\tau}{2}\partial_t H^*(\boldsymbol{x})\right) = P_h\left(H_0^* - \frac{\tau\mu_0^{-1}}{2}\nabla\times\widetilde{\boldsymbol{E}}_0\right), \tag{24c}$$

$$\tilde{H}_h^{\frac{1}{2}}(\boldsymbol{x}) = P_h\left(\tilde{H}_0(\boldsymbol{x}) + \frac{\tau}{2}\partial_t\tilde{H}(\boldsymbol{x})\right) = P_h\left(\tilde{H}_0 + \frac{\tau}{2}H_0\right), \tag{24d}$$

where $\Pi_c\boldsymbol{E}_0 \in U_h$ denotes the Nédélec interpolation operator, and P_h denotes the standard L^2 projection operator into the space V_h .

It is known that the following interpolation and projection error estimates hold true [27]:

$$\|\boldsymbol{E} - \Pi_c\boldsymbol{E}\| + \|\nabla\times(\boldsymbol{E} - \Pi_c\boldsymbol{E})\| \leq Ch^l\|\boldsymbol{E}\|_{H^l(curl,\Omega)}, \quad \forall \boldsymbol{E} \in H^l(curl,\Omega), \ l \geq 1, \tag{25}$$

$$\|H - P_hH\| \leq Ch^l\|H\|_{H^l(\Omega)}, \qquad \forall H \in H^l(\Omega), \ l \geq 1. \tag{26}$$

Here and in the rest of the paper, we denote $\|\cdot\|$ for the L^2 norm on Ω.

3.1 The unconditional stability analysis

This subsection is devoted to the unconditional stability analysis of our scheme (23a)-(23e).

Theorem 1 *Denote the discrete energy at time t_m as:*

$$\mathcal{E}_{te}^{disc}(t_m) := \varepsilon_0 \left(\|\widetilde{\boldsymbol{E}}_h^m\|^2 + \|\widetilde{\boldsymbol{E}}_h^m - \boldsymbol{E}_h^m\|^2 \right) + \|\mu_0^{\frac{1}{2}} H_h^{m+\frac{1}{2}} + \frac{\tau}{2\sqrt{\mu_0}} \nabla \times \widetilde{\boldsymbol{E}}_h^m\|^2 + \varepsilon_0^{-2}\mu_0 \|(\sigma_x\sigma_y)^{\frac{1}{2}} \widetilde{H}_h^{m+\frac{1}{2}}\|^2.$$

Then under the time step constraint

$$\tau \le \frac{\varepsilon_0}{3(\|\sigma_x\|_\infty + \|\sigma_y\|_\infty)}, \tag{27}$$

we have the following stability for the scheme (23a)-(23e)*: for any $m \ge 0$,*

$$\mathcal{E}_{te}^{disc}(t_m) \le \exp\left[4(\|\sigma_x\|_\infty + \|\sigma_y\|_\infty)\varepsilon_0^{-1}(m\tau)\right] \cdot \mathcal{E}_{te}^{disc}(t_0). \tag{28}$$

Remark 2 *We want to remark that the stability* (28) *is unconditionally stable, since the time step constraint* (27) *is independent of mesh size h. Furthermore, the stability* (28) *has exactly the same form as the following continuous stability established in our previous work [17, Theorem 1]:*

$$\mathcal{E}_{te}(t) \le \exp\left[4(\|\sigma_x\|_\infty + \|\sigma_y\|_\infty)\varepsilon_0^{-1} t\right] \cdot \mathcal{E}_{te}(t_0),$$

where the energy is denoted as:

$$\mathcal{E}_{te}(t) := \left[\varepsilon_0 \left(\|\widetilde{\boldsymbol{E}}\|^2 + \|\widetilde{\boldsymbol{E}} - \boldsymbol{E}\|^2 \right) + \|\mu_0^{\frac{1}{2}} H + \frac{\tau}{2\sqrt{\mu_0}} \nabla \times \widetilde{\boldsymbol{E}}\|^2 + \varepsilon_0^{-2}\mu_0 \|(\sigma_x\sigma_y)^{\frac{1}{2}} \widetilde{H}\|^2 \right](t).$$

Proof. Choosing $\boldsymbol{\phi_h} = \overline{\widetilde{\boldsymbol{E}}}_h^{n+\frac{1}{2}}$ in (23a) and $\psi_h = \overline{H}_h^{n+1}$ in (23c), and adding the results, we obtain:

$$\begin{aligned}
&\varepsilon_0 \left(\delta_\tau \boldsymbol{E}_h^{n+\frac{1}{2}}, \overline{\widetilde{\boldsymbol{E}}}_h^{n+\frac{1}{2}} \right) + \left(\Sigma^{**} \overline{\boldsymbol{E}}_h^{n+\frac{1}{2}}, \overline{\widetilde{\boldsymbol{E}}}_h^{n+\frac{1}{2}} \right) + \mu_0 \left(\delta_\tau H_h^{*,n+1}, \overline{H}_h^{n+1} \right) \\
&= \left(H_h^{n+\frac{1}{2}}, \nabla \times \overline{\widetilde{\boldsymbol{E}}}_h^{n+\frac{1}{2}} \right) - \left(\nabla \times \widetilde{\boldsymbol{E}}_h^{n+1}, \overline{H}_h^{n+1} \right) - \frac{\tau}{8\mu_0} \left(\|\nabla \times \widetilde{\boldsymbol{E}}_h^{n+1}\|^2 - \|\nabla \times \widetilde{\boldsymbol{E}}_h^n\|^2 \right) \\
&= \frac{1}{2} \left[\left(H_h^{n+\frac{1}{2}}, \nabla \times \widetilde{\boldsymbol{E}}_h^n \right) - \left(H_h^{n+\frac{3}{2}}, \nabla \times \widetilde{\boldsymbol{E}}_h^{n+1} \right) \right] - \frac{\tau}{8\mu_0} \left(\|\nabla \times \widetilde{\boldsymbol{E}}_h^{n+1}\|^2 - \|\nabla \times \widetilde{\boldsymbol{E}}_h^n\|^2 \right).
\end{aligned} \tag{29}$$

Choosing $\widetilde{\boldsymbol{\phi}}_h = \overline{\widetilde{\boldsymbol{E}}}_h^{n+\frac{1}{2}}$ in (23b) and $\widehat{\psi}_h = \mu_0 \overline{H}_h^{n+1}$ in (23e), respectively, we have

$$\frac{\varepsilon_0}{2\tau} \left(\|\widetilde{\boldsymbol{E}}_h^{n+1}\|^2 - \|\widetilde{\boldsymbol{E}}_h^n\|^2 \right) = \varepsilon_0 \left(\delta_\tau \boldsymbol{E}_h^{n+\frac{1}{2}}, \overline{\widetilde{\boldsymbol{E}}}_h^{n+\frac{1}{2}} \right) + \left(\Sigma_{**} \overline{\boldsymbol{E}}_h^{n+\frac{1}{2}}, \overline{\widetilde{\boldsymbol{E}}}_h^{n+\frac{1}{2}} \right), \tag{30}$$

and

$$\begin{aligned}
&\frac{\mu_0}{2\tau} \left(\|H_h^{n+\frac{3}{2}}\|^2 - \|H_h^{n+\frac{1}{2}}\|^2 \right) + \varepsilon_0^{-1}\mu_0 \|(\sigma_x + \sigma_y)^{\frac{1}{2}} \overline{H}_h^{n+1}\|^2 + \varepsilon_0^{-2}\mu_0 \left(\sigma_x\sigma_y \overline{\widetilde{H}}_h^{n+1}, \overline{H}_h^{n+1} \right) \\
= \; &\mu_0 \left(\delta_\tau H_h^{*,n+1}, \overline{H}_h^{n+1} \right).
\end{aligned} \tag{31}$$

Adding (29)-(31), we attain

$$\begin{aligned}
&\frac{\varepsilon_0}{2\tau} \left(\|\widetilde{\boldsymbol{E}}_h^{n+1}\|^2 - \|\widetilde{\boldsymbol{E}}_h^n\|^2 \right) + \frac{\mu_0}{2\tau} \left(\|H_h^{n+\frac{3}{2}}\|^2 - \|H_h^{n+\frac{1}{2}}\|^2 \right) + \varepsilon_0^{-1}\mu_0 \|(\sigma_x + \sigma_y)^{\frac{1}{2}} \overline{H}_h^{n+1}\|^2 \\
&+ \varepsilon_0^{-2}\mu_0 \left(\sigma_x\sigma_y \overline{\widetilde{H}}_h^{n+1}, \overline{H}_h^{n+1} \right) + \frac{\tau}{8\mu_0} \left(\|\nabla \times \widetilde{\boldsymbol{E}}_h^{n+1}\|^2 - \|\nabla \times \widetilde{\boldsymbol{E}}_h^n\|^2 \right) \\
&= \left((\Sigma_{**} - \Sigma^{**}) \overline{\boldsymbol{E}}_h^{n+\frac{1}{2}}, \overline{\widetilde{\boldsymbol{E}}}_h^{n+\frac{1}{2}} \right) + \frac{1}{2} \left[\left(H_h^{n+\frac{1}{2}}, \nabla \times \widetilde{\boldsymbol{E}}_h^n \right) - \left(H_h^{n+\frac{3}{2}}, \nabla \times \widetilde{\boldsymbol{E}}_h^{n+1} \right) \right].
\end{aligned} \tag{32}$$

Choosing $\widetilde{\psi}_h = \varepsilon_0^{-2}\mu_0\overline{\widetilde{H}}_h^{n+1}$ in (23d), and using it to replace the fourth term in (32), we have

$$\begin{aligned}
&\frac{\varepsilon_0}{2\tau}\left(\|\widetilde{\boldsymbol{E}}_h^{n+1}\|^2 - \|\widetilde{\boldsymbol{E}}_h^{n}\|^2\right) + \frac{\mu_0}{2\tau}\left(\|H_h^{n+\frac{3}{2}}\|^2 - \|H_h^{n+\frac{1}{2}}\|^2\right) + \varepsilon_0^{-1}\mu_0\|(\sigma_x+\sigma_y)^{\frac{1}{2}}\overline{\widetilde{H}}_h^{n+1}\|^2 \\
&+ \frac{\varepsilon_0^{-2}\mu_0}{2\tau}\left(\|(\sigma_x\sigma_y)^{\frac{1}{2}}\widetilde{H}_h^{n+\frac{3}{2}}\|^2 - \|(\sigma_x\sigma_y)^{\frac{1}{2}}\widetilde{H}_h^{n+\frac{1}{2}}\|^2\right) + \frac{\tau}{8\mu_0}\left(\|\nabla\times\widetilde{\boldsymbol{E}}_h^{n+1}\|^2 - \|\nabla\times\widetilde{\boldsymbol{E}}_h^{n}\|^2\right) \\
&= \left((\Sigma_{**}-\Sigma^{**})\overline{\boldsymbol{E}}_h^{n+\frac{1}{2}}, \overline{\widetilde{\boldsymbol{E}}}_h^{n+\frac{1}{2}}\right) + \frac{1}{2}\left[\left(H_h^{n+\frac{1}{2}}, \nabla\times\widetilde{\boldsymbol{E}}_h^{n}\right) - \left(H_h^{n+\frac{3}{2}}, \nabla\times\widetilde{\boldsymbol{E}}_h^{n+1}\right)\right].
\end{aligned} \tag{33}$$

Choosing $\widetilde{\boldsymbol{\phi}}_h = \overline{\widetilde{\boldsymbol{E}}_h^{n+\frac{1}{2}} - \boldsymbol{E}_h^{n+\frac{1}{2}}}$ in (23b), we obtain

$$\frac{\varepsilon_0}{2\tau}\left(\|\widetilde{\boldsymbol{E}}_h^{n+1} - \boldsymbol{E}_h^{n+1}\|^2 - \|\widetilde{\boldsymbol{E}}_h^{n} - \boldsymbol{E}_h^{n}\|^2\right) = \left(\Sigma_{**}\overline{\boldsymbol{E}}_h^{n+\frac{1}{2}}, \overline{\widetilde{\boldsymbol{E}}}_h^{n+\frac{1}{2}} - \overline{\boldsymbol{E}}_h^{n+\frac{1}{2}}\right). \tag{34}$$

Adding (33) and (34) together, then summing up from $n=0$ to m, we obtain

$$\begin{aligned}
&\frac{\varepsilon_0}{2}\left(\|\widetilde{\boldsymbol{E}}_h^{m+1}\|^2 - \|\widetilde{\boldsymbol{E}}_h^{0}\|\right) + \frac{\mu_0}{2}\left(\|H_h^{m+\frac{3}{2}}\|^2 - \|H_h^{\frac{1}{2}}\|^2\right) + \tau\varepsilon_0^{-1}\mu_0\sum_{n=0}^{m}\|(\sigma_x+\sigma_y)^{\frac{1}{2}}\overline{\widetilde{H}}_h^{n+1}\|^2 \\
&\quad + \frac{\varepsilon_0^{-2}\mu_0}{2}\left(\|(\sigma_x\sigma_y)^{\frac{1}{2}}\widetilde{H}_h^{m+\frac{3}{2}}\|^2 - \|(\sigma_x\sigma_y)^{\frac{1}{2}}\widetilde{H}_h^{\frac{1}{2}}\|^2\right) + \frac{\tau^2}{8\mu_0}\left(\|\nabla\times\widetilde{\boldsymbol{E}}_h^{m+1}\|^2 - \|\nabla\times\widetilde{\boldsymbol{E}}_h^{0}\|^2\right) \\
&\quad + \frac{\varepsilon_0}{2}\left(\|\widetilde{\boldsymbol{E}}_h^{m+1} - \boldsymbol{E}_h^{m+1}\|^2 - \|\widetilde{\boldsymbol{E}}_h^{0} - \boldsymbol{E}_h^{0}\|^2\right) \\
&= \tau\sum_{n=0}^{m}\left((\Sigma_{**}-\Sigma^{**})\overline{\boldsymbol{E}}_h^{n+\frac{1}{2}}, \overline{\widetilde{\boldsymbol{E}}}_h^{n+\frac{1}{2}}\right) + \frac{\tau}{2}\left[\left(H_h^{\frac{1}{2}}, \nabla\times\widetilde{\boldsymbol{E}}_h^{0}\right) - \left(H_h^{m+\frac{3}{2}}, \nabla\times\widetilde{\boldsymbol{E}}_h^{m+1}\right)\right] \\
&\quad + \tau\sum_{n=0}^{m}\left(\Sigma_{**}\overline{\boldsymbol{E}}_h^{n+\frac{1}{2}}, \overline{\widetilde{\boldsymbol{E}}}_h^{n+\frac{1}{2}} - \overline{\boldsymbol{E}}_h^{n+\frac{1}{2}}\right) := \sum_{i=1}^{3} Err_i.
\end{aligned} \tag{35}$$

Using inequalities $\left|\frac{a+b}{2}\right|^2 \le \frac{1}{2}(a^2+b^2)$ and $|a|^2 = |a-b+b|^2 \le 2(|a-b|^2+b^2)$, we have

$$\begin{aligned}
&\tau\left((\Sigma_{**}-\Sigma^{**})\overline{\boldsymbol{E}}_h^{n+\frac{1}{2}}, \overline{\widetilde{\boldsymbol{E}}}_h^{n+\frac{1}{2}}\right) \le \frac{\tau\varepsilon_0^{-1}\|\sigma_x-\sigma_y\|_\infty}{2}\left[\varepsilon_0\|\overline{\boldsymbol{E}}_h^{n+\frac{1}{2}}\|^2 + \varepsilon_0\|\overline{\widetilde{\boldsymbol{E}}}_h^{n+\frac{1}{2}}\|^2\right] \\
&= \frac{\tau\varepsilon_0^{-1}\|\sigma_x-\sigma_y\|_\infty}{2}\left[\varepsilon_0\|\overline{\boldsymbol{E}}_h^{n+\frac{1}{2}} - \overline{\widetilde{\boldsymbol{E}}}_h^{n+\frac{1}{2}} + \overline{\widetilde{\boldsymbol{E}}}_h^{n+\frac{1}{2}}\|^2 + \varepsilon_0\|\overline{\widetilde{\boldsymbol{E}}}_h^{n+\frac{1}{2}}\|^2\right] \\
&\le \tau\varepsilon_0^{-1}\|\sigma_x-\sigma_y\|_\infty\left[\varepsilon_0\|\overline{\boldsymbol{E}}_h^{n+\frac{1}{2}} - \overline{\widetilde{\boldsymbol{E}}}_h^{n+\frac{1}{2}}\|^2 + \frac{3}{2}\varepsilon_0\|\overline{\widetilde{\boldsymbol{E}}}_h^{n+\frac{1}{2}}\|^2\right] \\
&\le \tau\varepsilon_0^{-1}\|\sigma_x-\sigma_y\|_\infty\left[\frac{\varepsilon_0}{2}\left(\|\boldsymbol{E}_h^{n+1} - \widetilde{\boldsymbol{E}}_h^{n+1}\|^2 + \|\boldsymbol{E}_h^{n} - \widetilde{\boldsymbol{E}}_h^{n}\|^2\right) + \frac{3\varepsilon_0}{4}\left(\|\widetilde{\boldsymbol{E}}_h^{n+1}\|^2 + \|\widetilde{\boldsymbol{E}}_h^{n}\|^2\right)\right].
\end{aligned} \tag{36}$$

Similarly, we can obtain

$$\begin{aligned}
\tau\left(\Sigma_{**}\overline{\boldsymbol{E}}_h^{n+\frac{1}{2}}, \overline{\widetilde{\boldsymbol{E}}}_h^{n+\frac{1}{2}} - \overline{\boldsymbol{E}}_h^{n+\frac{1}{2}}\right) &= \tau\left(\Sigma_{**}(\overline{\boldsymbol{E}}_h^{n+\frac{1}{2}} - \overline{\widetilde{\boldsymbol{E}}}_h^{n+\frac{1}{2}}) + \Sigma_{**}\overline{\widetilde{\boldsymbol{E}}}_h^{n+\frac{1}{2}}, \overline{\widetilde{\boldsymbol{E}}}_h^{n+\frac{1}{2}} - \overline{\boldsymbol{E}}_h^{n+\frac{1}{2}}\right) \\
&\le \tau\varepsilon_0^{-1}\max(\|\sigma_x\|_\infty, \|\sigma_y\|_\infty)\left[\frac{\varepsilon_0}{2}\|\overline{\widetilde{\boldsymbol{E}}}_h^{n+\frac{1}{2}}\|^2 + \frac{\varepsilon_0}{2}\|\overline{\widetilde{\boldsymbol{E}}}_h^{n+\frac{1}{2}} - \overline{\boldsymbol{E}}_h^{n+\frac{1}{2}}\|^2\right] \\
&\le \tau\varepsilon_0^{-1}\max(\|\sigma_x\|_\infty, \|\sigma_y\|_\infty)\left[\frac{\varepsilon_0}{4}\left(\|\widetilde{\boldsymbol{E}}_h^{n+1}\|^2 + \|\widetilde{\boldsymbol{E}}_h^{n}\|^2\right)\right. \\
&\qquad \left. + \frac{\varepsilon_0}{4}\left(\|\widetilde{\boldsymbol{E}}_h^{n+1} - \boldsymbol{E}_h^{n+1}\|^2 + \|\widetilde{\boldsymbol{E}}_h^{n} - \boldsymbol{E}_h^{n}\|^2\right)\right].
\end{aligned} \tag{37}$$

where we used the estimate

$$\left(\Sigma_{**}(\overline{\boldsymbol{E}}_h^{n+\frac{1}{2}} - \overline{\widetilde{\boldsymbol{E}}}_h^{n+\frac{1}{2}}), \overline{\widetilde{\boldsymbol{E}}}_h^{n+\frac{1}{2}} - \overline{\boldsymbol{E}}_h^{n+\frac{1}{2}}\right) \le 0$$

to obtain the first inequality.

It is easy to check that the following identity holds true:

$$\|\sqrt{\mu_0}H_h^{m+\frac{3}{2}} + \frac{\tau}{2\sqrt{\mu_0}}\nabla\times\widetilde{\boldsymbol{E}}_h^{m+1}\|^2 = \mu_0\|H_h^{m+\frac{3}{2}}\|^2 + \tau\left(H_h^{m+\frac{3}{2}}, \nabla\times\widetilde{\boldsymbol{E}}_h^{m+1}\right) + \frac{\tau^2}{4\mu_0}\|\nabla\times\widetilde{\boldsymbol{E}}_h^{m+1}\|^2. \tag{38}$$

Substituting the above estimates (36)-(38) into (35), we have

$$\begin{aligned}
&\frac{\varepsilon_0}{2}\left(\|\widetilde{\boldsymbol{E}}_h^{m+1}\|^2 - \|\widetilde{\boldsymbol{E}}_h^0\|^2\right) + \frac{1}{2}\|\sqrt{\mu_0}H_h^{m+\frac{3}{2}} + \frac{\tau}{2\sqrt{\mu_0}}\nabla\times\widetilde{\boldsymbol{E}}_h^{m+1}\|^2 + \tau\varepsilon_0^{-1}\mu_0\sum_{n=0}^{m}\|(\sigma_x+\sigma_y)^{\frac{1}{2}}\overline{H}_h^{n+1}\|^2 \\
&\quad + \frac{\varepsilon_0^{-2}\mu_0}{2}\left(\|(\sigma_x\sigma_y)^{\frac{1}{2}}\widetilde{H}_h^{m+\frac{1}{2}}\|^2 - \|(\sigma_x\sigma_y)^{\frac{1}{2}}\widetilde{H}_h^{\frac{1}{2}}\|^2\right) + \frac{\varepsilon_0}{2}\left(\|\widetilde{\boldsymbol{E}}_h^{m+1} - \boldsymbol{E}_h^{m+1}\|^2 - \|\widetilde{\boldsymbol{E}}_h^0 - \boldsymbol{E}_h^0\|^2\right) \\
&\quad \le \tau\varepsilon_0^{-1}\|\sigma_x-\sigma_y\|_\infty\left[\frac{\varepsilon_0}{2}\|\boldsymbol{E}_h^{m+1} - \widetilde{\boldsymbol{E}}_h^{m+1}\|^2 + \frac{3\varepsilon_0}{4}\|\widetilde{\boldsymbol{E}}_h^{m+1}\|^2\right] \\
&\quad + \tau\varepsilon_0^{-1}\|\sigma_x-\sigma_y\|_\infty\sum_{n=0}^{m}\left[\varepsilon_0\|\boldsymbol{E}_h^n - \widetilde{\boldsymbol{E}}_h^n\|^2 + \frac{3\varepsilon_0}{2}\|\widetilde{\boldsymbol{E}}_h^n\|^2\right] \\
&\quad + \tau\varepsilon_0^{-1}\max(\|\sigma_x\|_\infty,\|\sigma_y\|_\infty)\left(\frac{\varepsilon_0}{4}\|\widetilde{\boldsymbol{E}}_h^{m+1}\|^2 + \frac{\varepsilon_0}{4}\|\widetilde{\boldsymbol{E}}_h^{m+1} - \boldsymbol{E}_h^{m+1}\|^2\right) \\
&\quad + \tau\varepsilon_0^{-1}\max(\|\sigma_x\|_\infty,\|\sigma_y\|_\infty)\sum_{n=0}^{m}\left[\frac{\varepsilon_0}{2}\|\widetilde{\boldsymbol{E}}_h^n\|^2 + \frac{\varepsilon_0}{2}\|\widetilde{\boldsymbol{E}}_h^n - \boldsymbol{E}_h^n\|^2\right] + \frac{1}{2}\|\sqrt{\mu_0}H_h^{\frac{1}{2}} + \frac{\tau}{2\sqrt{\mu_0}}\nabla\times\widetilde{\boldsymbol{E}}_h^0\|^2.
\end{aligned} \tag{39}$$

To get a nice stability result, now we relax the bound for those coefficients on the right hand side of ((39)) by the following simple estimates:

$$\|\sigma_x-\sigma_y\|_\infty \le \|\sigma_x\|_\infty + \|\sigma_y\|_\infty, \quad \max(\|\sigma_x\|_\infty,\|\sigma_y\|_\infty) \le \|\sigma_x\|_\infty + \|\sigma_y\|_\infty.$$

Using the following time step constraints (equivalent to (27)):

$$\tau\varepsilon_0^{-1}(\|\sigma_x\|_\infty + \|\sigma_y\|_\infty) \le \frac{1}{3},$$

dropping the nonnegative term of the left hand side of (39), then using the discrete Gronwall inequality, we have

$$\begin{aligned}
&\varepsilon_0\|\widetilde{\boldsymbol{E}}_h^{m+1}\|^2 + \|\mu_0^{\frac{1}{2}}H_h^{m+\frac{3}{2}} + \frac{\tau}{2\sqrt{\mu_0}}\nabla\times\widetilde{\boldsymbol{E}}_h^{m+1}\|^2 + \varepsilon_0^{-2}\mu_0\|(\sigma_x\sigma_y)^{\frac{1}{2}}\widetilde{H}_h^{m+\frac{3}{2}}\|^2 + \varepsilon_0\|\widetilde{\boldsymbol{E}}_h^{m+1} - \boldsymbol{E}_h^{m+1}\|^2 \\
&\quad \le \exp\left[4(\|\sigma_x\|_\infty + \|\sigma_y\|_\infty)\varepsilon_0^{-1}(m+1)\tau\right] \\
&\quad \cdot\left\{\varepsilon_0\left(\|\widetilde{\boldsymbol{E}}_h^0\|^2 + \|\widetilde{\boldsymbol{E}}_h^0 - \boldsymbol{E}_h^0\|^2\right) + \|\sqrt{\mu_0}H_h^{\frac{1}{2}} + \frac{\tau}{2\sqrt{\mu_0}}\nabla\times\widetilde{\boldsymbol{E}}_h^0\|^2 + \varepsilon_0^{-2}\mu_0\|(\sigma_x\sigma_y)^{\frac{1}{2}}\widetilde{H}_h^{\frac{1}{2}}\|^2\right\},
\end{aligned} \tag{40}$$

which completes the proof of (28). □

3.2 The convergence analysis

In this subsection, we will carry out the convergence analysis of our scheme (23a)-(23d). To accomplish that, we need the following lemma.

Lemma 1 *[22, Ch.3] Denote $u^n := u(\cdot, t_n)$. We have*

$$(i)\ \ \|\delta_\tau u^{n+\frac{1}{2}}\|^2 = \|\frac{u^{n+1}-u^n}{\tau}\|^2 \le \frac{1}{\tau}\int_{t_n}^{t_{n+1}}\|\partial_t u(t)\|^2\,dt, \quad \forall u \in H^1(0,T;L^2(\Omega)), \tag{41}$$

$$(ii)\ \ \|\overline{u}^{n+\frac{1}{2}} - \frac{1}{\tau}\int_{t_n}^{t_{n+1}}u(t)\,dt\|^2 \le \frac{\tau^3}{4}\int_{t_n}^{t_{n+1}}\|\partial_{tt}u(t)\|^2\,dt, \quad \forall u \in H^2(0,T;L^2(\Omega)), \tag{42}$$

$$(iii)\ \ \|u^{n+\frac{1}{2}} - \frac{1}{\tau}\int_{t_n}^{t_{n+1}}u(t)\,dt\|^2 \le \frac{\tau^3}{4}\int_{t_n}^{t_{n+1}}\|\partial_{tt}u(t)\|^2\,dt, \quad \forall u \in H^2(0,T;L^2(\Omega)). \tag{43}$$

To simplify the analysis, let us introduce the solution errors:

$$\begin{aligned}
\boldsymbol{\mathcal{E}}^n &= \boldsymbol{E}(t_n) - \boldsymbol{E}_h^n = (\boldsymbol{E}(t_n) - \Pi_c\boldsymbol{E}^n) + (\Pi_c\boldsymbol{E}^n - \boldsymbol{E}_h^n) := \boldsymbol{E}_\xi^n - \boldsymbol{E}_{h\eta}^n \\
\widetilde{\boldsymbol{\mathcal{E}}}^n &= \widetilde{\boldsymbol{E}}(t_n) - \widetilde{\boldsymbol{E}}_h^n = \left(\widetilde{\boldsymbol{E}}(t_n) - \Pi_c\widetilde{\boldsymbol{E}}^n\right) + \left(\Pi_c\widetilde{\boldsymbol{E}}^n - \widetilde{\boldsymbol{E}}_h^n\right) := \widetilde{\boldsymbol{E}}_\xi^n - \widetilde{\boldsymbol{E}}_{h\eta}^n \\
\mathcal{H}^{n+\frac{1}{2}} &= H(t_{n+\frac{1}{2}}) - H_h^{n+\frac{1}{2}} = \left(H(t_{n+\frac{1}{2}}) - P_hH^{n+\frac{1}{2}}\right) + \left(P_hH^{n+\frac{1}{2}} - H_h^{n+\frac{1}{2}}\right) := H_\xi^{n+\frac{1}{2}} - H_{h\eta}^{n+\frac{1}{2}} \\
\mathcal{H}^{*,n+\frac{1}{2}} &= H^*(t_{n+\frac{1}{2}}) - H_h^{*,n+\frac{1}{2}} = \left(H^*(t_{n+\frac{1}{2}}) - P_hH^{*,n+\frac{1}{2}}\right) + \left(P_hH^{*,n+\frac{1}{2}} - H_h^{*,n+\frac{1}{2}}\right) := H_\xi^{*,n+\frac{1}{2}} - H_{h\eta}^{*,n+\frac{1}{2}} \\
\widetilde{\mathcal{H}}^{n+\frac{1}{2}} &= \widetilde{H}(t_{n+\frac{1}{2}}) - \widetilde{H}_h^{n+\frac{1}{2}} = \left(\widetilde{H}(t_{n+\frac{1}{2}}) - P_h\widetilde{H}^{n+\frac{1}{2}}\right) + \left(P_h\widetilde{H}^{n+\frac{1}{2}} - \widetilde{H}_h^{n+\frac{1}{2}}\right) := \widetilde{H}_\xi^{n+\frac{1}{2}} - \widetilde{H}_{h\eta}^{n+\frac{1}{2}},
\end{aligned}$$

where $\Pi_c\boldsymbol{E}$ and $\Pi_c\widetilde{E} \in U_h$ denote the Nédélec intepolations, P_hH, P_hH^*, and $P_h\widetilde{H} \in V_h$ denote the standard L^2 projections.

To establish the error estimate for scheme (23a)-(23e), we first derive the error equations.

Integrating (1a),(1b) from t_n to t_{n+1} and integrating (1c)-(1e) from $t_{n+\frac{1}{2}}$ to $t_{n+\frac{3}{2}}$, and multiplying the corresponding results by $\frac{1}{\tau}\boldsymbol{\phi}_h, \frac{1}{\tau}\widetilde{\boldsymbol{\phi}}_h, \frac{1}{\tau}\psi_h, \frac{1}{\tau}\sigma_x\sigma_y\widetilde{\psi}_h, \widehat{\psi}_h$, respectively, and integrating over Ω, we obtain

$$\varepsilon_0\left(\delta_\tau\boldsymbol{E}^{n+\frac{1}{2}}, \boldsymbol{\phi}_h\right) + \left(\tfrac{1}{\tau}\textstyle\int_{t_n}^{t_{n+1}}\Sigma^{**}\boldsymbol{E}(s)\,ds, \boldsymbol{\phi}_h\right) = \left(\tfrac{1}{\tau}\textstyle\int_{t_n}^{t_{n+1}}H(s)\,ds, \nabla\times\boldsymbol{\phi}_h\right), \tag{44}$$

$$\varepsilon_0\left(\delta_\tau\widetilde{\boldsymbol{E}}^{n+\frac{1}{2}}, \widetilde{\boldsymbol{\phi}}_h\right) = \varepsilon_0\left(\delta_\tau\boldsymbol{E}^{n+\frac{1}{2}}, \widetilde{\boldsymbol{\phi}}_h\right) + \left(\tfrac{1}{\tau}\textstyle\int_{t_n}^{t_{n+1}}\Sigma_{**}\boldsymbol{E}(s)\,ds, \widetilde{\boldsymbol{\phi}}_h\right), \tag{45}$$

$$\mu_0\left(\delta_\tau H^{*,n+1}, \psi_h\right) = -\left(\tfrac{1}{\tau}\textstyle\int_{t_{n+\frac{1}{2}}}^{t_{n+\frac{3}{2}}}\nabla\times\widetilde{\boldsymbol{E}}(s)\,ds, \psi_h\right), \tag{46}$$

$$\left(\delta_\tau\widetilde{H}^{n+1}, \sigma_x\sigma_y\widetilde{\psi}_h\right) = \left(\tfrac{1}{\tau}\textstyle\int_{t_{n+\frac{1}{2}}}^{t_{n+\frac{3}{2}}}H(s)\,ds, \sigma_x\sigma_y\widetilde{\psi}_h\right), \tag{47}$$

$$\begin{aligned}
&\left(\delta_\tau H^{n+1}, \widehat{\psi}_h\right) + \varepsilon_0^{-1}\left(\tfrac{1}{\tau}\textstyle\int_{t_{n+\frac{1}{2}}}^{t_{n+\frac{3}{2}}}(\sigma_x+\sigma_y)H(s)\,ds, \widehat{\psi}_h\right) \\
&\qquad + \varepsilon_0^{-2}\left(\tfrac{1}{\tau}\textstyle\int_{t_{n+\frac{1}{2}}}^{t_{n+\frac{3}{2}}}\sigma_x\sigma_y\widetilde{H}(s)\,ds, \widehat{\psi}_h\right) = \left(\delta_\tau H^{*,n+1}, \widehat{\psi}_h\right).
\end{aligned} \tag{48}$$

Subtracting (44) from (23a), we obtain the first error equation:

$$\begin{aligned}
&\varepsilon_0\left(\delta_\tau\boldsymbol{E}_{h\eta}^{n+\frac{1}{2}}, \boldsymbol{\phi}_h\right) + \left(\Sigma^{**}\overline{\boldsymbol{E}}_{h\eta}^{n+\frac{1}{2}}, \boldsymbol{\phi}_{\boldsymbol{h}}\right) - \left(H_{h\eta}^{n+\frac{1}{2}}, \nabla\times\boldsymbol{\phi}_h\right) + \frac{\tau^2}{4\mu_0}\left(\nabla\times\delta_\tau\widetilde{\boldsymbol{E}}_{h\eta}^{n+\frac{1}{2}}, \nabla\times\boldsymbol{\phi}_h\right) \\
&= \varepsilon_0\left(\delta_\tau\boldsymbol{E}_\xi^{n+\frac{1}{2}}, \boldsymbol{\phi}_h\right) + \left(\frac{1}{\tau}\int_{t_n}^{t_{n+1}}\Sigma^{**}\boldsymbol{E}(s)\,ds - \Sigma^{**}\Pi_c\overline{\boldsymbol{E}}^{n+\frac{1}{2}}, \boldsymbol{\phi}_{\boldsymbol{h}}\right) \\
&\quad + \left(P_hH^{n+\frac{1}{2}} - \frac{1}{\tau}\int_{t_n}^{t_{n+1}}H(s)\,ds, \nabla\times\boldsymbol{\phi}_{\boldsymbol{h}}\right) - \frac{\tau^2}{4\mu_0}\left(\nabla\times\delta_\tau\Pi_c\widetilde{\boldsymbol{E}}^{n+\frac{1}{2}}, \nabla\times\boldsymbol{\phi}_{\boldsymbol{h}}\right).
\end{aligned} \tag{49}$$

Subtracting (45) from (23b), we have the 2nd error equation:

$$\begin{aligned}
&\varepsilon_0\left(\delta_\tau\widetilde{\boldsymbol{E}}_{h\eta}^{n+\frac{1}{2}}, \widetilde{\boldsymbol{\phi}}_h\right) - \varepsilon_0\left(\delta_\tau\boldsymbol{E}_{h\eta}^{n+\frac{1}{2}}, \widetilde{\boldsymbol{\phi}}_h\right) - \left(\Sigma_{**}\overline{\boldsymbol{E}}_{h\eta}^{n+\frac{1}{2}}, \widetilde{\boldsymbol{\phi}}_h\right) \\
&= \varepsilon_0\left(\delta_\tau\widetilde{\boldsymbol{E}}_\xi^{n+\frac{1}{2}}, \widetilde{\boldsymbol{\phi}}_h\right) - \varepsilon_0\left(\delta_\tau\boldsymbol{E}_\xi^{n+\frac{1}{2}}, \widetilde{\boldsymbol{\phi}}_h\right) + \left(\Sigma_{**}\Pi_c\overline{\boldsymbol{E}}^{n+\frac{1}{2}} - \frac{1}{\tau}\int_{t_n}^{t_{n+1}}\Sigma_{**}\boldsymbol{E}(s)\,ds, \widetilde{\boldsymbol{\phi}}_h\right).
\end{aligned} \tag{50}$$

Similarly, subtracting (46) from (23c), we obtain the 3rd error equation:

$$\begin{aligned}
&\mu_0\left(\delta_\tau H_{h\eta}^{*,n+1}, \psi_h\right) + \left(\nabla\times\widetilde{E}_{h\eta}^{n+1}, \psi_h\right) \\
&\quad = \mu_0\left(\delta_\tau H_\xi^{*,n+1}, \psi_h\right) + \left(\frac{1}{\tau}\int_{t_{n+\frac{1}{2}}}^{t_{n+\frac{3}{2}}}\left(\nabla\times\widetilde{E}(s) - \nabla\times\Pi_c\widetilde{\boldsymbol{E}}^{n+1}\right)ds, \psi_h\right).
\end{aligned} \tag{51}$$

Subtracting (47) from (23d), we obtain the 4th error equation:

$$\left(\delta_\tau \widetilde{H}_{h\eta}^{n+1}, \sigma_x\sigma_y\widetilde{\psi}_h\right) - \left(\overline{H}_{h\eta}^{n+1}, \sigma_x\sigma_y\widetilde{\psi}_h\right) = \left(\delta_\tau \widetilde{H}_{\xi}^{n+1}, \sigma_x\sigma_y\widetilde{\psi}_h\right) + \left(P_h\overline{H}^{n+1} - \frac{1}{\tau}\int_{t_{n+\frac{1}{2}}}^{t_{n+\frac{3}{2}}} H(s)\,ds, \sigma_x\sigma_y\widetilde{\psi}_h\right). \quad (52)$$

Subtracting (48) from (23e), we obtain the 5th error equation:

$$\begin{aligned}
&\left(\delta_\tau H_{h\eta}^{n+1}, \widehat{\psi}_h\right) + \varepsilon_0^{-1}\left((\sigma_x+\sigma_y)\overline{H}_{h\eta}^{n+1}, \widehat{\psi}_h\right) + \varepsilon_0^{-2}\left(\sigma_x\sigma_y\overline{\widetilde{H}}_{h\eta}^{n+1}, \widehat{\psi}_h\right) - \left(\delta_\tau H_{h\eta}^{*,n+1}, \widehat{\psi}_h\right) \\
&= \left(\delta_\tau H_{\xi}^{n+1}, \widehat{\psi}_h\right) + \varepsilon_0^{-1}\left(\frac{1}{\tau}\int_{t_{n+\frac{1}{2}}}^{t_{n+\frac{3}{2}}} (\sigma_x+\sigma_y)\left(H(s) - P_h\overline{H}^{n+1}\right) ds, \widehat{\psi}_h\right) \\
&\quad + \varepsilon_0^{-2}\left(\frac{1}{\tau}\int_{t_{n+\frac{1}{2}}}^{t_{n+\frac{3}{2}}} \sigma_x\sigma_y\left(\widetilde{H}(s) - P_h\overline{\widetilde{H}}^{n+1}\right) ds, \widehat{\psi}_h\right) - \left(\delta_\tau H_{\xi}^{*,n+1}, \widehat{\psi}_h\right).
\end{aligned} \quad (53)$$

With the above preparations, we can prove the following optimal error estimate for the scheme (23a)-(23e).

Theorem 2 *Under the following regularity assumptions:*

$$\boldsymbol{E},\ \widetilde{\boldsymbol{E}},\ \nabla\times\widetilde{\boldsymbol{E}} \in L^\infty(0,T;H^l(curl,\Omega)), \quad H,\ \widetilde{H} \in L^\infty(0,T;H^l(\Omega)), \quad (54a)$$

$$\partial_{tt}\boldsymbol{E},\ \nabla\times\partial_{tt}\widetilde{\boldsymbol{E}},\ \partial_{tt}H,\ \nabla\times\partial_{tt}H,\ \partial_{tt}\widetilde{H} \in L^2(0,T;L^2(\Omega)), \quad (54b)$$

$$\partial_t\boldsymbol{E},\ \partial_t\widetilde{\boldsymbol{E}},\ \nabla\times\partial_t\widetilde{\boldsymbol{E}} \in L^2(0,T;H^l(curl,\Omega)), \quad \partial_t\widetilde{H} \in L^2(0,T;H^l(\Omega)), \quad (54c)$$

then we have: for any $0 \le m \le N_t - 2$,

$$\begin{aligned}
&\varepsilon_0^{\frac{1}{2}}\left[\|\widetilde{\boldsymbol{\mathcal{E}}}^{m+1}\| + \|\widetilde{\boldsymbol{\mathcal{E}}}^{m+1} - \boldsymbol{\mathcal{E}}^{m+1}\|\right] + \|\sqrt{\mu_0}\mathcal{H}^{m+\frac{3}{2}} + \frac{\tau}{2\sqrt{\mu_0}}\nabla\times\widetilde{\boldsymbol{\mathcal{E}}}^{m+1}\| + \varepsilon_0^{-1}\mu_0^{\frac{1}{2}}\|(\sigma_x\sigma_y)^{\frac{1}{2}}\widetilde{\mathcal{H}}^{m+\frac{3}{2}}\| \\
&\le C(h^l + \tau^2),
\end{aligned} \quad (55)$$

where the constant $C > 0$ is independent of h and τ.

Proof. Choosing $\boldsymbol{\phi_h} = \overline{\widetilde{\boldsymbol{E}}}_{h\eta}^{n+\frac{1}{2}}$ in (49) and $\psi_h = \overline{H}_{h\eta}^{n+1}$ in (51), then adding the results together, we have

$$\begin{aligned}
&\varepsilon_0\left(\delta_\tau\boldsymbol{E}_{h\eta}^{n+\frac{1}{2}}, \overline{\widetilde{\boldsymbol{E}}}_{h\eta}^{n+\frac{1}{2}}\right) + \left(\Sigma^{**}\overline{\boldsymbol{E}}_{h\eta}^{n+\frac{1}{2}}, \overline{\widetilde{\boldsymbol{E}}}_{h\eta}^{n+\frac{1}{2}}\right) + \mu_0\left(\delta_\tau H_{h\eta}^{*,n+1}, \overline{H}_{h\eta}^{n+1}\right) - \varepsilon_0\left(\delta_\tau\boldsymbol{E}_{\xi}^{n+\frac{1}{2}}, \overline{\widetilde{\boldsymbol{E}}}_{h\eta}^{n+\frac{1}{2}}\right) \\
&= \frac{1}{2}\left[\left(H_{h\eta}^{n+\frac{1}{2}}, \nabla\times\widetilde{\boldsymbol{E}}_{h\eta}^{n}\right) - \left(H_{h\eta}^{n+\frac{3}{2}}, \nabla\times\widetilde{\boldsymbol{E}}_{h\eta}^{n+1}\right)\right] - \frac{\tau}{8\mu_0}\left(\|\nabla\times\widetilde{\boldsymbol{E}}_{h\eta}^{n+1}\|^2 - \|\nabla\times\widetilde{\boldsymbol{E}}_{h\eta}^{n}\|^2\right) \\
&\quad + \left(\frac{1}{\tau}\int_{t_n}^{t_{n+1}} \Sigma^{**}\left(\boldsymbol{E}(s) - \Pi_c\overline{\boldsymbol{E}}^{n+\frac{1}{2}}\right) ds, \overline{\widetilde{\boldsymbol{E}}}_{h\eta}^{n+\frac{1}{2}}\right) + \left(\frac{1}{\tau}\int_{t_n}^{t_{n+1}} \left(P_hH^{n+\frac{1}{2}} - H(s)\right) ds, \nabla\times\overline{\widetilde{\boldsymbol{E}}}_{h\eta}^{n+\frac{1}{2}}\right) \\
&\quad - \frac{\tau^2}{4\mu_0}\left(\nabla\times\delta_\tau\Pi_c\widetilde{\boldsymbol{E}}^{n+\frac{1}{2}}, \nabla\times\overline{\widetilde{\boldsymbol{E}}}_{h\eta}^{n+\frac{1}{2}}\right) + \left(\frac{1}{\tau}\int_{t_{n+\frac{1}{2}}}^{t_{n+\frac{3}{2}}} \nabla\times\left(\widetilde{\boldsymbol{E}}(s) - \Pi_c\widetilde{\boldsymbol{E}}^{n+1}\right) ds, \overline{H}_{h\eta}^{n+1}\right) \\
&:= \sum_{i=1}^{6} Est_i,
\end{aligned} \quad (56)$$

where we use the L^2 projection property $\left(\delta_\tau H_{\xi}^{*,n+1}, \overline{H}_{h\eta}^{n+1}\right) = 0$, and the identity

$$\left(H_{h\eta}^{n+\frac{1}{2}}, \nabla\times\overline{\widetilde{\boldsymbol{E}}}_{h\eta}^{n+\frac{1}{2}}\right) - \left(\nabla\times\widetilde{\boldsymbol{E}}_{h\eta}^{n+1}, \overline{H}_{h\eta}^{n+1}\right) = \frac{1}{2}\left[\left(H_{h\eta}^{n+\frac{1}{2}}, \nabla\times\widetilde{\boldsymbol{E}}_{h\eta}^{n}\right) - \left(H_{h\eta}^{n+\frac{3}{2}}, \nabla\times\widetilde{\boldsymbol{E}}_{h\eta}^{n+1}\right)\right].$$

Choosing $\widetilde{\boldsymbol{\phi}}_h = \overline{\widetilde{\boldsymbol{E}}}_{h\eta}^{n+\frac{1}{2}}$ in (50) and $\widehat{\psi}_h = \mu_0 \overline{H}_{h\eta}^{n+1}$ in (53), respectively, we have

$$\begin{aligned}
&\frac{\varepsilon_0}{2\tau}\left(\|\widetilde{\boldsymbol{E}}_{h\eta}^{n+1}\|^2 - \|\widetilde{\boldsymbol{E}}_{h\eta}^{n}\|^2\right) - \varepsilon_0\left(\delta_\tau \boldsymbol{E}_{h\eta}^{n+\frac{1}{2}}, \overline{\widetilde{\boldsymbol{E}}}_{h\eta}^{n+\frac{1}{2}}\right) - \left(\Sigma_{**}\overline{\boldsymbol{E}}_{h\eta}^{n+\frac{1}{2}}, \overline{\widetilde{\boldsymbol{E}}}_{h\eta}^{n+\frac{1}{2}}\right) + \varepsilon_0\left(\delta_\tau \boldsymbol{E}_{\xi}^{n+\frac{1}{2}}, \overline{\widetilde{\boldsymbol{E}}}_{h\eta}^{n+\frac{1}{2}}\right)\\
&\quad = \varepsilon_0\left(\delta_\tau \widetilde{\boldsymbol{E}}_{\xi}^{n+\frac{1}{2}}, \overline{\widetilde{\boldsymbol{E}}}_{h\eta}^{n+\frac{1}{2}}\right) + \left(\frac{1}{\tau}\int_{t_n}^{t_{n+1}} \Sigma_{**}\left(\Pi_c \overline{\boldsymbol{E}}^{n+\frac{1}{2}} - \boldsymbol{E}(s)\right) ds, \overline{\widetilde{\boldsymbol{E}}}_{h\eta}^{n+\frac{1}{2}}\right)\\
&\quad := Est_7 + Est_8,
\end{aligned} \tag{57}$$

and

$$\begin{aligned}
&\frac{\mu_0}{2\tau}\left(\|H_{h\eta}^{n+\frac{3}{2}}\|^2 - \|H_{h\eta}^{n+\frac{1}{2}}\|^2\right) + \varepsilon_0^{-1}\mu_0\|(\sigma_x+\sigma_y)^{\frac{1}{2}}\overline{H}_{h\eta}^{n+1}\|^2 + \varepsilon_0^{-2}\mu_0\left(\sigma_x\sigma_y \overline{\widetilde{H}}_{h\eta}^{n+1}, \overline{H}_{h\eta}^{n+1}\right) - \mu_0\left(\delta_\tau H_{h\eta}^{*,n+1}, \overline{H}_{h\eta}^{n+1}\right)\\
&\quad = \varepsilon_0^{-1}\mu_0\left(\frac{1}{\tau}\int_{t_{n+\frac{1}{2}}}^{t_{n+\frac{3}{2}}} (\sigma_x+\sigma_y)\left(H(s) - P_h\overline{H}^{n+1}\right) ds, \overline{H}_{h\eta}^{n+1}\right)\\
&\qquad + \varepsilon_0^{-2}\mu_0\left(\frac{1}{\tau}\int_{t_{n+\frac{1}{2}}}^{t_{n+\frac{3}{2}}} \sigma_x\sigma_y\left(\widetilde{H}(s) - P_h\overline{\widetilde{H}}^{n+1}\right) ds, \overline{H}_{h\eta}^{n+1}\right) := Est_9 + Est_{10},
\end{aligned} \tag{58}$$

where we dropped the following two zero terms by the L^2 projection property:

$$\mu_0\left(\delta_\tau H_{\xi}^{n+1}, \overline{H}_{h\eta}^{n+1}\right), \quad \mu_0\left(\delta_\tau H_{\xi}^{*,n+1}, \overline{H}_{h\eta}^{n+1}\right) = 0.$$

Choosing $\widetilde{\psi}_h = \varepsilon_0^{-2}\mu_0 \overline{\widetilde{H}}_{h\eta}^{n+1}$ in (52), we have

$$\begin{aligned}
&\frac{\varepsilon_0^{-2}\mu_0}{2\tau}\left(\|(\sigma_x\sigma_y)^{\frac{1}{2}}\widetilde{H}_{h\eta}^{n+\frac{3}{2}}\|^2 - \|(\sigma_x\sigma_y)^{\frac{1}{2}}\widetilde{H}_{h\eta}^{n+\frac{1}{2}}\|^2\right) - \varepsilon_0^{-2}\mu_0\left(\overline{H}_{h\eta}^{n+1}, \sigma_x\sigma_y\overline{\widetilde{H}}_{h\eta}^{n+1}\right)\\
&= \varepsilon_0^{-2}\mu_0\left(\delta_\tau \widetilde{H}_{\xi}^{n+1}, \sigma_x\sigma_y\overline{\widetilde{H}}_{h\eta}^{n+1}\right) - \varepsilon_0^{-2}\mu_0\left(\frac{1}{\tau}\int_{t_{n+\frac{1}{2}}}^{t_{n+\frac{3}{2}}}\left(H(s) - P_h\overline{H}^{n+1}\right) ds, \sigma_x\sigma_y\overline{\widetilde{H}}_{h\eta}^{n+1}\right) := Est_{11} + Est_{12}.
\end{aligned} \tag{59}$$

Adding (56)-(59) together, we have

$$\begin{aligned}
&\frac{\varepsilon_0}{2\tau}\left(\|\widetilde{\boldsymbol{E}}_{h\eta}^{n+1}\|^2 - \|\widetilde{\boldsymbol{E}}_{h\eta}^{n}\|^2\right) + \frac{\mu_0}{2\tau}\left(\|H_{h\eta}^{n+\frac{3}{2}}\|^2 - \|H_{h\eta}^{n+\frac{1}{2}}\|^2\right) + \varepsilon_0^{-1}\mu_0\|(\sigma_x+\sigma_y)^{\frac{1}{2}}\overline{H}_{h\eta}^{n+1}\|^2\\
&\quad + \frac{\varepsilon_0^{-2}\mu_0}{2\tau}\left(\|(\sigma_x\sigma_y)^{\frac{1}{2}}\widetilde{H}_{h\eta}^{n+\frac{3}{2}}\|^2 - \|(\sigma_x\sigma_y)^{\frac{1}{2}}\widetilde{H}_{h\eta}^{n+\frac{1}{2}}\|^2\right) + \frac{\tau}{8\mu_0}\left(\|\nabla\times\widetilde{\boldsymbol{E}}_{h\eta}^{n+1}\|^2 - \|\nabla\times\widetilde{\boldsymbol{E}}_{h\eta}^{n}\|^2\right)\\
&\quad = \left((\Sigma_{**} - \Sigma^{**})\overline{\boldsymbol{E}}_{h\eta}^{n+\frac{1}{2}}, \overline{\widetilde{\boldsymbol{E}}}_{h\eta}^{n+\frac{1}{2}}\right) + \frac{1}{2}\left[\left(H_{h\eta}^{n+\frac{1}{2}}, \nabla\times\widetilde{\boldsymbol{E}}_{h\eta}^{n}\right) - \left(H_{h\eta}^{n+\frac{3}{2}}, \nabla\times\widetilde{\boldsymbol{E}}_{h\eta}^{n+1}\right)\right] + \sum_{i=3}^{12} Est_i.
\end{aligned} \tag{60}$$

Choosing $\widetilde{\boldsymbol{\phi}} = \overline{\widetilde{\boldsymbol{E}}}_{h\eta}^{n+\frac{1}{2}} - \overline{\boldsymbol{E}}_{h\eta}^{n+\frac{1}{2}}$ in (50), we obtain

$$\begin{aligned}
&\frac{\varepsilon_0}{2\tau}\left(\|\widetilde{\boldsymbol{E}}_{h\eta}^{n+1} - \boldsymbol{E}_{h\eta}^{n+1}\|^2 - \|\widetilde{\boldsymbol{E}}_{h\eta}^{n} - \boldsymbol{E}_{h\eta}^{n}\|^2\right) - \left(\Sigma_{**}\overline{\boldsymbol{E}}_{h\eta}^{n+\frac{1}{2}}, \overline{\widetilde{\boldsymbol{E}}}_{h\eta}^{n+\frac{1}{2}} - \overline{\boldsymbol{E}}_{h\eta}^{n+\frac{1}{2}}\right)\\
&\quad = \varepsilon_0\left(\delta_\tau(\widetilde{\boldsymbol{E}}_{\xi}^{n+\frac{1}{2}} - \boldsymbol{E}_{\xi}^{n+\frac{1}{2}}), \overline{\widetilde{\boldsymbol{E}}}_{h\eta}^{n+\frac{1}{2}} - \overline{\boldsymbol{E}}_{h\eta}^{n+\frac{1}{2}}\right)\\
&\qquad + \left(\frac{1}{\tau}\int_{t_n}^{t_{n+1}} \Sigma_{**}\left(\Pi_c\overline{\boldsymbol{E}}^{n+\frac{1}{2}} - \boldsymbol{E}(s)\right) ds, \overline{\widetilde{\boldsymbol{E}}}_{h\eta}^{n+\frac{1}{2}} - \overline{\boldsymbol{E}}_{h\eta}^{n+\frac{1}{2}}\right) := Est_{13} + Est_{14}.
\end{aligned} \tag{61}$$

Adding (60) and (61) together, then summing up the result from $n=0$ to m, we obtain

$$
\begin{aligned}
&\frac{\varepsilon_0}{2}\left(\|\widetilde{\boldsymbol{E}}_{h\eta}^{m+1}\|^2-\|\widetilde{\boldsymbol{E}}_{h\eta}^{0}\|^2\right)+\frac{\mu_0}{2}\left(\|H_{h\eta}^{m+\frac{3}{2}}\|^2-\|H_{h\eta}^{\frac{1}{2}}\|^2\right)+\tau\varepsilon_0^{-1}\mu_0\sum_{n=0}^{m}\|(\sigma_x+\sigma_y)^{\frac{1}{2}}\overline{H}_{h\eta}^{n+1}\|^2\\
&\quad+\frac{\varepsilon_0^{-2}\mu_0}{2}\left(\|(\sigma_x\sigma_y)^{\frac{1}{2}}\widetilde{H}_{h\eta}^{m+\frac{3}{2}}\|^2-\|(\sigma_x\sigma_y)^{\frac{1}{2}}\widetilde{H}_{h\eta}^{\frac{1}{2}}\|^2\right)+\frac{\tau^2}{8\mu_0}\left(\|\nabla\times\widetilde{\boldsymbol{E}}_{h\eta}^{m+1}\|^2-\|\nabla\times\widetilde{\boldsymbol{E}}_{h\eta}^{0}\|^2\right)\\
&\quad+\frac{\varepsilon_0}{2}\left(\|\widetilde{\boldsymbol{E}}_{h\eta}^{m+1}-\boldsymbol{E}_{h\eta}^{m+1}\|^2-\|\widetilde{\boldsymbol{E}}_{h\eta}^{0}-\boldsymbol{E}_{h\eta}^{0}\|^2\right)\\
&=\tau\sum_{n=0}^{m}\left((\Sigma_{**}-\Sigma^{**})\overline{\boldsymbol{E}}_{h\eta}^{n+\frac{1}{2}},\overline{\widetilde{\boldsymbol{E}}}_{h\eta}^{n+\frac{1}{2}}\right)+\frac{\tau}{2}\left[\left(H_{h\eta}^{\frac{1}{2}},\nabla\times\widetilde{\boldsymbol{E}}_{h\eta}^{0}\right)-\left(H_{h\eta}^{m+\frac{3}{2}},\nabla\times\widetilde{\boldsymbol{E}}_{h\eta}^{m+1}\right)\right]\\
&\quad+\tau\sum_{n=0}^{m}\left(\Sigma_{**}\overline{\boldsymbol{E}}_{h\eta}^{n+\frac{1}{2}},\overline{\widetilde{\boldsymbol{E}}}_{h\eta}^{n+\frac{1}{2}}-\overline{\boldsymbol{E}}_{h\eta}^{n+\frac{1}{2}}\right)+\tau\sum_{n=0}^{m}\sum_{i=3}^{14}Est_i.
\end{aligned}
\tag{62}
$$

Now we need to bound those right hand side terms of (62). First, similar to (36) and (37) in the stability analysis, respectively, we have

$$
\begin{aligned}
\tau\sum_{n=0}^{m}\left((\Sigma_{**}-\Sigma^{**})\overline{\boldsymbol{E}}_{h\eta}^{n+\frac{1}{2}},\overline{\widetilde{\boldsymbol{E}}}_{h\eta}^{n+\frac{1}{2}}\right)&\le\tau\varepsilon_0^{-1}(\|\sigma_x\|_\infty+\|\sigma_y\|_\infty)\sum_{n=0}^{m}\Big[\frac{3\varepsilon_0}{4}\left(\|\widetilde{\boldsymbol{E}}_{h\eta}^{n+1}\|^2+\|\widetilde{\boldsymbol{E}}_{h\eta}^{n}\|^2\right)\\
&\quad+\frac{\varepsilon_0}{2}\left(\|\boldsymbol{E}_{h\eta}^{n+1}-\widetilde{\boldsymbol{E}}_{h\eta}^{n+1}\|^2+\|\boldsymbol{E}_{h\eta}^{n}-\widetilde{\boldsymbol{E}}_{h\eta}^{n}\|^2\right)\Big],
\end{aligned}
\tag{63}
$$

and

$$
\begin{aligned}
\tau\sum_{n=0}^{m}\left(\Sigma_{**}\overline{\boldsymbol{E}}_{h\eta}^{n+\frac{1}{2}},\overline{\widetilde{\boldsymbol{E}}}_{h\eta}^{n+\frac{1}{2}}-\overline{\boldsymbol{E}}_{h\eta}^{n+\frac{1}{2}}\right)&\le\tau\varepsilon_0^{-1}(\|\sigma_x\|_\infty+\|\sigma_y\|_\infty)\sum_{n=0}^{m}\Big[\frac{\varepsilon_0}{4}\left(\|\widetilde{\boldsymbol{E}}_{h\eta}^{n+1}\|^2+\|\widetilde{\boldsymbol{E}}_{h\eta}^{n}\|^2\right)\\
&\quad+\frac{\varepsilon_0}{4}\left(\|\widetilde{\boldsymbol{E}}_{h\eta}^{n+1}-\boldsymbol{E}_{h}^{n+1}\|^2+\|\widetilde{\boldsymbol{E}}_{h\eta}^{n}-\boldsymbol{E}_{h\eta}^{n}\|^2\right)\Big].
\end{aligned}
\tag{64}
$$

Moving the second right hand side term of (62) to combine with some left hand side terms, we have

$$
\begin{aligned}
&\frac{\mu_0}{2}\|H_{h\eta}^{m+\frac{3}{2}}\|^2+\frac{\tau}{2}\left(H_{h\eta}^{m+\frac{3}{2}},\nabla\times\widetilde{\boldsymbol{E}}_{h\eta}^{m+1}\right)+\frac{\tau^2}{8\mu_0}\|\nabla\times\widetilde{\boldsymbol{E}}_{h\eta}^{m+1}\|^2\\
&=\frac{1}{2}\|\sqrt{\mu_0}H_{h\eta}^{m+\frac{3}{2}}+\frac{\tau}{2\sqrt{\mu_0}}\nabla\times\widetilde{\boldsymbol{E}}_{h\eta}^{m+1}\|^2.
\end{aligned}
\tag{65}
$$

Now we need to estimate the rest right hand side items in (62). Using the arithmetic-geometric mean inequality

$$
(a,b)\le\delta\|a\|^2+\frac{1}{4\delta}\|b\|^2,\qquad\forall\,\delta>0,
\tag{66}
$$

the inequality $\|\frac{a+b}{2}\|^2\le\frac{1}{2}(\|a\|^2+\|b\|^2)$, Lemma 1 and the interpolation error estimate, we have

$$
\begin{aligned}
\tau\sum_{n=0}^{m}Est_3&=\tau\sum_{n=0}^{m}\left(\left(\frac{1}{\tau}\int_{t_n}^{t_{n+1}}\boldsymbol{E}(s)ds-\boldsymbol{E}^{n+\frac{1}{2}}+\boldsymbol{E}^{n+\frac{1}{2}}-\Pi_c\boldsymbol{E}^{n+\frac{1}{2}}\right),\Sigma^{**}\overline{\widetilde{\boldsymbol{E}}}_{h\eta}^{n+\frac{1}{2}}\right)\\
&\le\tau\sum_{n=0}^{m}(\|\sigma_x\|_\infty+\|\sigma_y\|_\infty)\left[\delta_3\|\overline{\widetilde{\boldsymbol{E}}}_{h\eta}^{n+\frac{1}{2}}\|^2+\frac{1}{2\delta_3}\left(\|\frac{1}{\tau}\int_{t_n}^{t_{n+1}}\boldsymbol{E}(s)ds-\boldsymbol{E}^{n+\frac{1}{2}}\|^2+\|\boldsymbol{E}_\xi^{n+\frac{1}{2}}\|^2\right)\right]\\
&\le\tau\sum_{n=0}^{m}(\|\sigma_x\|_\infty+\|\sigma_y\|_\infty)\Bigg[\frac{\delta_3}{2}\left(\|\widetilde{\boldsymbol{E}}_{h\eta}^{n+1}\|^2+\|\widetilde{\boldsymbol{E}}_{h\eta}^{n}\|^2\right)\\
&\quad+\frac{1}{2\delta_3}\left(\frac{\tau^3}{4}\int_{t_n}^{t_{n+1}}\|\partial_{tt}\boldsymbol{E}\|^2\,dt+Ch^{2l}\|\boldsymbol{E}^{n+\frac{1}{2}}\|^2_{H^l(curl;\Omega)}\right)\Bigg].
\end{aligned}
\tag{67}
$$

Let us introduce the wave propagation speed notation $C_v=\frac{1}{\sqrt{\varepsilon_0\mu_0}}$. Using the fact that

$$
\left(P_hH^{n+\frac{1}{2}}-H^{n+\frac{1}{2}},\nabla\times\overline{\widetilde{\boldsymbol{E}}}_{h\eta}^{n+\frac{1}{2}}\right)=0,
$$

integration by parts and Lemma 1, we have

$$\begin{aligned}\tau\sum_{n=0}^{m} Est_4 &= \tau\sum_{n=0}^{m}\left(\frac{1}{\tau}\int_{t_n}^{t_{n+1}}\left(H^{n+\frac{1}{2}}-H(s)\right)ds, \nabla\times\overline{\widetilde{\boldsymbol{E}}}_{h\eta}^{n+\frac{1}{2}}\right)\\ &= \tau\sum_{n=0}^{m}\left(\frac{1}{\tau}\int_{t_n}^{t_{n+1}}\nabla\times\left(H^{n+\frac{1}{2}}-H(s)\right)ds, \overline{\widetilde{\boldsymbol{E}}}_{h\eta}^{n+\frac{1}{2}}\right)\\ &\le \tau C_v\sum_{n=0}^{m}\left[\varepsilon_0\delta_4\|\overline{\widetilde{\boldsymbol{E}}}_{h\eta}^{n+\frac{1}{2}}\|^2+\frac{\mu_0}{4\delta_4}\cdot\frac{\tau^3}{4}\int_{t_n}^{t_{n+1}}\|\nabla\times\partial_{tt}H\|^2\,dt\right]\\ &\le \tau C_v\sum_{n=0}^{m}\left[\frac{\delta_4\varepsilon_0}{2}\left(\|\widetilde{\boldsymbol{E}}_{h\eta}^{n+1}\|^2+\|\widetilde{\boldsymbol{E}}_{h\eta}^{n}\|^2\right)+\frac{\mu_0}{4\delta_4}\cdot\frac{\tau^3}{4}\int_{t_n}^{t_{n+1}}\|\nabla\times\partial_{tt}H\|^2\,dt\right].\end{aligned}\tag{68}$$

Using integration by parts, Lemma 1 and the interpolation error estimate, we obtain

$$\begin{aligned}\tau\sum_{n=0}^{m} Est_5 &= -\frac{\tau^3}{4\mu_0}\sum_{n=0}^{m}\left(\nabla\times\delta_\tau\Pi_c\widetilde{\boldsymbol{E}}^{n+\frac{1}{2}}, \nabla\times\overline{\widetilde{\boldsymbol{E}}}_{h\eta}^{n+\frac{1}{2}}\right)\\ &= \frac{\tau^3C_v^2}{4}\sum_{n=0}^{m}\varepsilon_0\left[\left(\delta_\tau\nabla\times\left(\widetilde{\boldsymbol{E}}^{n+\frac{1}{2}}-\Pi_c\widetilde{\boldsymbol{E}}^{n+\frac{1}{2}}\right), \nabla\times\overline{\widetilde{\boldsymbol{E}}}_{h\eta}^{n+\frac{1}{2}}\right)-\left(\delta_\tau\nabla\times\nabla\times\widetilde{\boldsymbol{E}}^{n+\frac{1}{2}}, \overline{\widetilde{\boldsymbol{E}}}_{h\eta}^{n+\frac{1}{2}}\right)\right]\\ &\le \sum_{n=0}^{m}\frac{1}{4\delta_5}\left(\frac{\tau^2C_v^2}{4}\right)^2\int_{t_n}^{t_{n+1}}\varepsilon_0h^{-2}\|\partial_t\nabla\times\left(\widetilde{\boldsymbol{E}}-\Pi_c\widetilde{\boldsymbol{E}}\right)\|^2dt+\tau\sum_{n=0}^{m}\delta_5\varepsilon_0h^2\|\nabla\times\overline{\widetilde{\boldsymbol{E}}}_{h\eta}^{n+\frac{1}{2}}\|^2\\ &\quad+\sum_{n=0}^{m}\frac{1}{4\delta_5}\left(\frac{\tau^2C_v^2}{4}\right)^2\int_{t_n}^{t_{n+1}}\varepsilon_0\|\partial_t\nabla\times\nabla\times\widetilde{\boldsymbol{E}}\|^2dt+\tau\sum_{n=0}^{m}\delta_5\varepsilon_0\|\overline{\widetilde{\boldsymbol{E}}}_{h\eta}^{n+\frac{1}{2}}\|^2\\ &\le \sum_{n=0}^{m}\frac{\tau^4C_v^4}{32\delta_5}\int_{t_n}^{t_{n+1}}\varepsilon_0\left(Ch^{2(l-1)}\|\nabla\times\partial_t\widetilde{\boldsymbol{E}}\|^2_{H^l(curl,\Omega)}+\|\nabla\times\nabla\times\partial_t\widetilde{\boldsymbol{E}}\|^2\right)dt\\ &\quad+\tau(C_{inv}^2+1)\sum_{n=0}^{m}\frac{\delta_5\varepsilon_0}{2}\left(\|\widetilde{\boldsymbol{E}}_{h\eta}^{n+1}\|^2+\|\widetilde{\boldsymbol{E}}_{h\eta}^{n}\|^2\right),\end{aligned}\tag{69}$$

where in the last step we used the standard inverse estimate [22, Ch.3]: $\|\nabla\times\overline{\widetilde{\boldsymbol{E}}}_{h\eta}^{n+\frac{1}{2}}\|\le C_{inv}h^{-1}\|\overline{\widetilde{\boldsymbol{E}}}_{h\eta}^{n+\frac{1}{2}}\|$.

Similarly, we have

$$\begin{aligned}&\tau\sum_{n=0}^{m} Est_6 = \tau\sum_{n=0}^{m}\left(\frac{1}{\tau}\int_{t_{n+\frac{1}{2}}}^{t_{n+\frac{3}{2}}}\nabla\times\left(\widetilde{\boldsymbol{E}}(s)-\Pi_c\widetilde{\boldsymbol{E}}^{n+1}\right)ds, \overline{H}_{h\eta}^{n+1}\right)\\ &\le \tau C_v\sum_{n=0}^{m}\left[\frac{\varepsilon_0}{4\delta_6}\|\frac{1}{\tau}\int_{t_{n+\frac{1}{2}}}^{t_{n+\frac{3}{2}}}\nabla\times\left(\widetilde{\boldsymbol{E}}(s)-\widetilde{\boldsymbol{E}}^{n+1}\right)ds+\nabla\times\left(\widetilde{\boldsymbol{E}}^{n+1}-\Pi_c\widetilde{\boldsymbol{E}}^{n+1}\right)\|^2+\mu_0\delta_6\|\overline{H}_{h\eta}^{n+1}\|^2\right]\\ &\le \tau C_v\sum_{n=0}^{m}\frac{\varepsilon_0}{2\delta_6}\left(\frac{\tau^3}{4}\int_{t_{n+\frac{1}{2}}}^{t_{n+\frac{3}{2}}}\|\nabla\times\partial_{tt}\widetilde{\boldsymbol{E}}\|^2\,dt+Ch^{2l}\|\widetilde{\boldsymbol{E}}^{n+1}\|^2_{H^l(curl;\Omega)}\right)+\tau C_v\delta_6\sum_{n=0}^{m}\mu_0\|\overline{H}_{h\eta}^{n+1}\|^2.\end{aligned}\tag{70}$$

By Lemma 1 and the interpolation error estimate, we have

$$\begin{aligned}\tau\sum_{n=0}^{m} Est_7 &= \tau\sum_{n=0}^{m}\varepsilon_0\left(\delta_\tau\widetilde{\boldsymbol{E}}_\xi^{n+\frac{1}{2}}, \overline{\widetilde{\boldsymbol{E}}}_{h\eta}^{n+\frac{1}{2}}\right)\\ &\le \tau\sum_{n=0}^{m}\frac{\delta_7\varepsilon_0}{2}\left(\|\widetilde{\boldsymbol{E}}_{h\eta}^{n+1}\|^2+\|\widetilde{\boldsymbol{E}}_{h\eta}^{n}\|^2\right)+\frac{\varepsilon_0}{4\delta_7}\int_0^{t_{m+1}}Ch^{2l}\|\partial_t\widetilde{\boldsymbol{E}}\|^2_{H^l(curl,\Omega)}\,dt.\end{aligned}\tag{71}$$

Similar to the analysis of Est_3, we easily obtain

$$\begin{aligned}\tau\sum_{n=0}^{m}Est_8&=\tau\sum_{n=0}^{m}\left(\frac{1}{\tau}\int_{t_n}^{t_{n+1}}\left[\left(\Pi_c\overline{\boldsymbol{E}}^{n+\frac{1}{2}}-\overline{\boldsymbol{E}}^{n+\frac{1}{2}}\right)+\left(\overline{\boldsymbol{E}}^{n+\frac{1}{2}}-\boldsymbol{E}(s)\right)\right]ds,\Sigma_{**}\overline{\widetilde{\boldsymbol{E}}}_{h\eta}^{n+\frac{1}{2}}\right)\\&\leq\tau\sum_{n=0}^{m}(\|\sigma_x\|_\infty+\|\sigma_y\|_\infty)\Bigg[\frac{\delta_8}{2}\left(\|\widetilde{\boldsymbol{E}}_{h\eta}^{n+1}\|^2+\|\widetilde{\boldsymbol{E}}_{h\eta}^{n}\|^2\right)\\&\quad+\frac{1}{2\delta_8}\left(\frac{\tau^3}{4}\int_{t_n}^{t_{n+1}}\|\partial_{tt}\boldsymbol{E}\|^2\,dt+Ch^{2l}\|\overline{\boldsymbol{E}}^{n+\frac{1}{2}}\|^2_{H^l(curl;\Omega)}\right)\Bigg].\end{aligned}\tag{72}$$

Similarly, we can obtain

$$\begin{aligned}\tau\sum_{n=0}^{m}Est_9&=\tau\sum_{n=0}^{m}\varepsilon_0^{-1}\mu_0\left(\frac{1}{\tau}\int_{t_{n+\frac{1}{2}}}^{t_{n+\frac{3}{2}}}(\sigma_x+\sigma_y)\left(H(s)-P_h\overline{H}^{n+1}\right)ds,\overline{H}_{h\eta}^{n+1}\right)\\&\leq\frac{\tau\varepsilon_0^{-1}\mu_0}{2}\sum_{n=0}^{m}\|(\sigma_x+\sigma_y)^{\frac{1}{2}}\overline{H}_{h\eta}^{n+1}\|^2\\&\quad+\frac{1}{2}\tau(\|\sigma_x\|_\infty+\|\sigma_y\|_\infty)\varepsilon_0^{-1}\mu_0\sum_{n=0}^{m}\left\|\left(\frac{1}{\tau}\int_{t_{n+\frac{1}{2}}}^{t_{n+\frac{3}{2}}}H(s)ds-\overline{H}^{n+1}\right)+\left(\overline{H}^{n+1}-P_h\overline{H}^{n+1}\right)\right\|^2\\&\leq\frac{\tau\varepsilon_0^{-1}\mu_0}{2}\sum_{n=0}^{m}\|(\sigma_x+\sigma_y)^{\frac{1}{2}}\overline{H}_{h\eta}^{n+1}\|^2\\&\quad+\tau(\|\sigma_x\|_\infty+\|\sigma_y\|_\infty)\varepsilon_0^{-1}\mu_0\sum_{n=0}^{m}\left[\frac{\tau^3}{4}\int_{t_{n+\frac{1}{2}}}^{t_{n+\frac{3}{2}}}\|\partial_{tt}H\|^2\,dt+Ch^{2l}\|\overline{H}^{n+1}\|^2_{H^l(\Omega)}\right],\end{aligned}\tag{73}$$

and

$$\begin{aligned}\tau\sum_{n=0}^{m}Est_{10}&=\tau\sum_{n=0}^{m}\varepsilon_0^{-2}\mu_0\left(\frac{1}{\tau}\int_{t_{n+\frac{1}{2}}}^{t_{n+\frac{3}{2}}}\sigma_x\sigma_y\left(\widetilde{H}(s)-P_h\overline{\widetilde{H}}^{n+1}\right)ds,\overline{H}_{h\eta}^{n+1}\right)\\&\leq\tau\|\sigma_x\|_\infty\|\sigma_y\|_\infty\varepsilon_0^{-2}\sum_{n=0}^{m}\Bigg[\delta_{10}\mu_0\|\overline{H}_{h\eta}^{n+1}\|^2\\&\quad+\frac{\mu_0}{2\delta_{10}}\left(\frac{\tau^3}{4}\int_{t_{n+\frac{1}{2}}}^{t_{n+\frac{3}{2}}}\|\partial_{tt}\widetilde{H}\|^2\,dt+Ch^{2l}\|\widetilde{H}^{n+1}\|^2_{H^l(\Omega)}\right)\Bigg].\end{aligned}\tag{74}$$

By Lemma 1 and the projection error estimate, we have

$$\begin{aligned}\tau\sum_{n=0}^{m}Est_{11}&=\tau\sum_{n=0}^{m}\varepsilon_0^{-2}\mu_0\left(\delta_\tau\widetilde{H}_\xi^{n+1},\sigma_x\sigma_y\overline{\widetilde{H}}_{h\eta}^{n+1}\right)\\&\leq\tau\varepsilon_0^{-2}\mu_0\sum_{n=0}^{m}\frac{\delta_{11}}{2}\left(\|(\sigma_x\sigma_y)^{\frac{1}{2}}\widetilde{H}_{h\eta}^{n+\frac{3}{2}}\|^2+\|(\sigma_x\sigma_y)^{\frac{1}{2}}\widetilde{H}_{h\eta}^{n+\frac{1}{2}}\|^2\right)\\&\quad+\varepsilon_0^{-2}\|\sigma_x\|_\infty\|\sigma_y\|_\infty\frac{1}{4\delta_{11}}\int_{t_{\frac{1}{2}}}^{t_{m+\frac{3}{2}}}Ch^{2l}\mu_0\|\partial_t\widetilde{H}\|^2_{H^l(\Omega)}dt.\end{aligned}\tag{75}$$

Similar to Est_{10}, we obtain

$$\begin{aligned}\tau\sum_{n=0}^{m}Est_{12}&=\tau\sum_{n=0}^{m}\varepsilon_0^{-2}\mu_0\left(\frac{1}{\tau}\int_{t_{n+\frac{1}{2}}}^{t_{n+\frac{3}{2}}}\left(H(s)-P_h\overline{H}^{n+1}\right)ds,\sigma_x\sigma_y\overline{\widetilde{H}}_{h\eta}^{n+1}\right)\\&\leq\tau\varepsilon_0^{-2}\mu_0\sum_{n=0}^{m}\frac{\delta_{12}}{2}\left(\|(\sigma_x\sigma_y)^{\frac{1}{2}}\widetilde{H}_{h\eta}^{n+\frac{3}{2}}\|^2+\|(\sigma_x\sigma_y)^{\frac{1}{2}}\widetilde{H}_{h\eta}^{n+\frac{1}{2}}\|^2\right)\\&\quad+\tau\varepsilon_0^{-2}\|\sigma_x\|_\infty\|\sigma_y\|_\infty\frac{1}{2\delta_{12}}\sum_{n=0}^{m}\left[\frac{\tau^3}{4}\int_{t_{n+\frac{1}{2}}}^{t_{n+\frac{3}{2}}}\mu_0\|\partial_{tt}H\|^2\,dt+Ch^{2l}\mu_0\|\overline{H}^{n+1}\|_{H^l(\Omega)}^2\right].\end{aligned}\tag{76}$$

Finally, by Lemma 1 and the interpolation error estimate, we have

$$\begin{aligned}\tau\sum_{n=0}^{m}Est_{13}&=\tau\sum_{n=0}^{m}\varepsilon_0\left(\delta_\tau(\widetilde{\boldsymbol{E}}_\xi^{n+\frac{1}{2}}-\boldsymbol{E}_\xi^{n+\frac{1}{2}}),\overline{\widetilde{\boldsymbol{E}}}_{h\eta}^{n+\frac{1}{2}}-\overline{\boldsymbol{E}}_{h\eta}^{n+\frac{1}{2}}\right)\\&\leq\tau\sum_{n=0}^{m}\frac{\delta_{13}\varepsilon_0}{2}\left(\|\widetilde{\boldsymbol{E}}_{h\eta}^{n+1}-\boldsymbol{E}_{h\eta}^{n+1}\|^2+\|\widetilde{\boldsymbol{E}}_{h\eta}^{n}-\boldsymbol{E}_{h\eta}^{n}\|^2\right)\\&\quad+\frac{1}{4\delta_{13}}\int_0^{t_{m+1}}Ch^{2l}\cdot\varepsilon_0\|\partial_t(\widetilde{\boldsymbol{E}}-\boldsymbol{E})\|_{H^l(curl,\Omega)}^2\,dt,\end{aligned}\tag{77}$$

and

$$\begin{aligned}\tau\sum_{n=0}^{m}Est_{14}&=\tau\sum_{n=0}^{m}\left(\frac{1}{\tau}\int_{t_n}^{t_{n+1}}\Sigma_{**}\left(\Pi_c\overline{\boldsymbol{E}}^{n+\frac{1}{2}}-\boldsymbol{E}(s)\right)ds,\overline{\widetilde{\boldsymbol{E}}}_{h\eta}^{n+\frac{1}{2}}-\overline{\boldsymbol{E}}_{h\eta}^{n+\frac{1}{2}}\right)\\&\leq\tau(\|\sigma_x\|_\infty+\|\sigma_y\|_\infty)\sum_{n=0}^{m}\left[\frac{\delta_{14}}{2}\left(\|\widetilde{\boldsymbol{E}}_{h\eta}^{n+1}-\boldsymbol{E}_{h\eta}^{n+1}\|^2+\|\widetilde{\boldsymbol{E}}_{h\eta}^{n}-\boldsymbol{E}_{h\eta}^{n}\|^2\right)\right.\\&\quad\left.+\frac{1}{2\delta_{14}}\left(\frac{\tau^3}{4}\int_{t_n}^{t_{n+1}}\|\partial_{tt}\boldsymbol{E}\|^2\,dt+Ch^{2l}\|\overline{\boldsymbol{E}}^{n+\frac{1}{2}}\|_{H^l(curl;\Omega)}^2\right)\right].\end{aligned}\tag{78}$$

Substituting the estimates (63)-(78) into (62), and combining many like terms, we obtain

$$
\begin{aligned}
&\frac{\varepsilon_0}{2}\left(\|\widetilde{\boldsymbol{E}}_{h\eta}^{m+1}\|^2-\|\widetilde{\boldsymbol{E}}_{h\eta}^{0}\|^2\right)+\frac{1}{2}\left(\|\sqrt{\mu_0}H_{h\eta}^{m+\frac{3}{2}}+\frac{\tau}{2\sqrt{\mu_0}}\nabla\times\widetilde{\boldsymbol{E}}_{h\eta}^{m+1}\|^2-\|\sqrt{\mu_0}H_{h\eta}^{\frac{1}{2}}+\frac{\tau}{2\sqrt{\mu_0}}\nabla\times\widetilde{\boldsymbol{E}}_{h\eta}^{0}\|^2\right)\\
&\quad+\tau\varepsilon_0^{-1}\mu_0\sum_{n=0}^{m}\|(\sigma_x+\sigma_y)^{\frac{1}{2}}\overline{H}_{h\eta}^{n+1}\|^2+\frac{\varepsilon_0^{-2}\mu_0}{2}\left(\|(\sigma_x\sigma_y)^{\frac{1}{2}}\widetilde{H}_{h\eta}^{m+\frac{3}{2}}\|^2-\|(\sigma_x\sigma_y)^{\frac{1}{2}}\widetilde{H}_{h\eta}^{\frac{1}{2}}\|^2\right)\\
&\quad+\frac{\varepsilon_0}{2}\left(\|\widetilde{\boldsymbol{E}}_{h\eta}^{m+1}-\boldsymbol{E}_{h\eta}^{m+1}\|^2-\|\widetilde{\boldsymbol{E}}_{h\eta}^{0}-\boldsymbol{E}_{h\eta}^{0}\|^2\right)\\
&\le\left[\varepsilon_0^{-1}(\|\sigma_x\|_\infty+\|\sigma_y\|_\infty)(1+\frac{\delta_3+\delta_8}{2})+\frac{1}{2}(C_v\delta_4+\delta_7)+\frac{1}{2}(C_{inv}^2+1)\delta_5\right]\cdot\tau\sum_{n=0}^{m}\varepsilon_0\left(\|\widetilde{\boldsymbol{E}}_{h\eta}^{n+1}\|^2+\|\widetilde{\boldsymbol{E}}_{h\eta}^{n}\|^2\right)\\
&\quad+\left[\varepsilon_0^{-1}(\|\sigma_x\|_\infty+\|\sigma_y\|_\infty)(1+\frac{\delta_{14}}{2})+\frac{\delta_{13}}{2}\right]\cdot\tau\sum_{n=0}^{m}\varepsilon_0\left(\|\boldsymbol{E}_{h\eta}^{n+1}-\widetilde{\boldsymbol{E}}_{h\eta}^{n+1}\|^2+\|\boldsymbol{E}_{h\eta}^{n}-\widetilde{\boldsymbol{E}}_{h\eta}^{n}\|^2\right)\\
&\quad+\left\{\left(C_v\varepsilon_0\delta_6+\varepsilon_0^{-1}\|\sigma_x\|_\infty\|\sigma_y\|_\infty\delta_{10}\right)\cdot\tau\varepsilon_0^{-1}\mu_0\sum_{n=0}^{m}\|\overline{H}_{h\eta}^{n+1}\|^2+\frac{\tau\varepsilon_0^{-1}\mu_0}{2}\sum_{n=0}^{m}\|(\sigma_x+\sigma_y)^{\frac{1}{2}}\overline{H}_{h\eta}^{n+1}\|^2\right\}\\
&\quad+(\delta_{11}+\delta_{12})\tau\sum_{n=0}^{m}\frac{\varepsilon_0^{-2}\mu_0}{2}\left(\|(\sigma_x\sigma_y)^{\frac{1}{2}}\widetilde{H}_{h\eta}^{n+\frac{3}{2}}\|^2+\|(\sigma_x\sigma_y)^{\frac{1}{2}}\widetilde{H}_{h\eta}^{n+\frac{1}{2}}\|^2\right)\\
&\quad+\tau^4\left\{(\|\sigma_x\|_\infty+\|\sigma_y\|_\infty)\left(\frac{1}{8\delta_3}+\frac{1}{8\delta_8}+\frac{1}{8\delta_{14}}\right)\int_0^{t_{m+1}}\|\partial_{tt}\boldsymbol{E}\|^2\,dt+\frac{C_v\mu_0}{16\delta_4}\int_0^{t_{m+1}}\|\nabla\times\partial_{tt}H\|^2\,dt\right.\\
&\quad+\frac{C_v^4}{32\delta_5}\int_0^{t_{m+1}}\varepsilon_0\left(Ch^{2(l-1)}\|\nabla\times\partial_t\widetilde{\boldsymbol{E}}\|_{H^l(curl,\Omega)}^2+\|\nabla\times\nabla\times\partial_t\widetilde{\boldsymbol{E}}\|^2\right)dt\\
&\quad+\frac{C_v}{8\delta_6}\int_{t_{\frac{1}{2}}}^{t_{m+\frac{3}{2}}}\varepsilon_0\|\nabla\times\partial_{tt}\widetilde{\boldsymbol{E}}\|^2\,dt+\left(\frac{\varepsilon_0^{-1}(\|\sigma_x\|_\infty+\|\sigma_y\|_\infty)}{4}+\frac{\varepsilon_0^{-2}\|\sigma_x\|_\infty\|\sigma_y\|_\infty}{8\delta_{12}}\right)\int_{t_{\frac{1}{2}}}^{t_{m+\frac{3}{2}}}\mu_0\|\partial_{tt}H\|^2\,dt\\
&\quad\left.+\frac{\varepsilon_0^{-2}\|\sigma_x\|_\infty\|\sigma_y\|_\infty}{8\delta_{10}}\int_{t_{\frac{1}{2}}}^{t_{m+\frac{3}{2}}}\mu_0\|\partial_{tt}\widetilde{H}\|^2\,dt\right\}\\
&\quad+Ch^{2l}\left\{\frac{1}{\delta_7}\int_0^{t_{m+1}}\varepsilon_0\|\partial_t\widetilde{\boldsymbol{E}}\|_{H^l(curl,\Omega)}^2\,dt+\frac{1}{\delta_{13}}\int_0^{t_{m+1}}\varepsilon_0\|\partial_t(\widetilde{\boldsymbol{E}}-\boldsymbol{E})\|_{H^l(curl,\Omega)}^2\,dt\right\}\\
&\quad+Ch^{2l}(m+1)\tau\left\{\left((\|\sigma_x\|_\infty+\|\sigma_y\|_\infty)(\frac{1}{\delta_3}+\frac{1}{\delta_8})+\frac{1}{\delta_{14}}\right)\|\boldsymbol{E}\|_{L^\infty(0,T;H^l(curl,\Omega))}^2+\frac{C_v}{\delta_6}\|\nabla\times\widetilde{\boldsymbol{E}}\|_{L^\infty(0,T;H^l(curl,\Omega))}^2\right.\\
&\quad\left.+\left(1+\frac{1}{\delta_{12}}\right)\|H\|_{L^\infty(0,T;H^l(\Omega))}^2+\frac{1}{\delta_{10}}\|\widetilde{H}\|_{L^\infty(0,T;H^l(\Omega))}^2+\frac{1}{\delta_{11}}\int_{t_{\frac{1}{2}}}^{t_{m+\frac{3}{2}}}\|\partial_t\widetilde{H}\|_{H^l(\Omega)}^2\,dt\right\}.
\end{aligned}
\tag{79}
$$

Now first choosing those δ_i small enough, then choosing τ small enough (but independent of mesh size h), dropping term $\tau\varepsilon_0^{-1}\mu_0\sum_{n=0}^{m}\|(\sigma_x+\sigma_y)^{\frac{1}{2}}\overline{H}_{h\eta}^{n+1}\|^2$, and using the discrete Gronwall inequality and the fact that $(m+1)\tau\le T$, we have

$$
\begin{aligned}
&\frac{\varepsilon_0}{2}\left[\|\widetilde{\boldsymbol{E}}_{h\eta}^{m+1}\|^2+\|\widetilde{\boldsymbol{E}}_{h\eta}^{m+1}-\boldsymbol{E}_{h\eta}^{m+1}\|^2\right]+\frac{1}{2}\|\sqrt{\mu_0}H_{h\eta}^{m+\frac{3}{2}}+\frac{\tau}{2\sqrt{\mu_0}}\nabla\times\widetilde{\boldsymbol{E}}_{h\eta}^{m+1}\|^2+\frac{\varepsilon_0^{-2}\mu_0}{2}\|(\sigma_x\sigma_y)^{\frac{1}{2}}\widetilde{H}_{h\eta}^{m+\frac{3}{2}}\|^2\\
&\le C\left\{\frac{\varepsilon_0}{2}\left[\|\widetilde{\boldsymbol{E}}_{h\eta}^{0}\|^2+\|\widetilde{\boldsymbol{E}}_{h\eta}^{0}-\boldsymbol{E}_{h\eta}^{0}\|^2\right]+\frac{1}{2}\|\sqrt{\mu_0}H_{h\eta}^{\frac{1}{2}}+\frac{\tau}{2\sqrt{\mu_0}}\nabla\times\widetilde{\boldsymbol{E}}_{h\eta}^{0}\|^2+\frac{\varepsilon_0^{-2}\mu_0}{2}\|(\sigma_x\sigma_y)^{\frac{1}{2}}\widetilde{H}_{h\eta}^{\frac{1}{2}}\|^2\right\}\\
&\qquad+Ch^{2l}+C\tau^4\le C(h^l+\tau^2)^2,
\end{aligned}
\tag{80}
$$

where in the last step, we used the initial approximations (24a)-(24d). Then by the triangular inequality, and the interpolation and projection error estimates, we immediately have

$$
\begin{aligned}
&\varepsilon_0^{\frac{1}{2}}\left[\|\widetilde{\boldsymbol{\mathcal{E}}}^{m+1}\|+\|\widetilde{\boldsymbol{\mathcal{E}}}^{m+1}-\boldsymbol{\mathcal{E}}^{m+1}\|\right]+\|\sqrt{\mu_0}\mathcal{H}^{m+\frac{3}{2}}+\frac{\tau}{2\sqrt{\mu_0}}\nabla\times\widetilde{\boldsymbol{\mathcal{E}}}^{m+1}\|+\varepsilon_0^{-1}\mu_0^{\frac{1}{2}}\|(\sigma_x\sigma_y)^{\frac{1}{2}}\widetilde{\mathcal{H}}^{m+\frac{3}{2}}\|\\
&\qquad\le C(h^l+\tau^2),
\end{aligned}
\tag{81}
$$

which completes the proof of (55). □

4 Numerical results

In this section, we present some numerical results to demonstrate the performance of our proposed leapfrog scheme. For simplity, we only implement the lowest order RTN mixed finite element spaces ($l = 1$) on triangular elements:

$$\begin{aligned}
\boldsymbol{V}_h &= \left\{\psi_h \in L^2(\Omega) : \psi_h|_K = \text{constant}, \forall K \in T_h\right\},\\
\boldsymbol{U}_h &= \left\{\boldsymbol{\phi}_h \in H(\text{curl};\Omega) : \boldsymbol{\phi}_h|_K = \text{span}\{\lambda_i \nabla \lambda_j - \lambda_j \nabla \lambda_i\}, \forall K \in T_h\right\},
\end{aligned}$$

where λ_i are the barycentric coordinate functions.

Example 1. This example is used to justify the convergence rate of our scheme. For this example, we choose the physical domain $\Omega = [0,1]^2$ and

$$\varepsilon_0 = \mu_0 = 1, \quad \sigma_x(x) = \pi(1 + \sin(\pi x)), \quad \sigma_y(y) = \pi(1 + \sin(\pi y)).$$

To construct an analytical solution, we add extra source terms to the model equations (1a)-(1e). More specifically, we solve the following governing equations:

$$\varepsilon_0 \partial_t \boldsymbol{E} + \Sigma^{**} \boldsymbol{E} = \nabla \times H + \boldsymbol{g}, \tag{82a}$$

$$\varepsilon_0 \partial_t \widetilde{\boldsymbol{E}} = \varepsilon_0 \partial_t \boldsymbol{E} + \Sigma_{**} \boldsymbol{E}, \tag{82b}$$

$$\mu_0 \partial_t H^* = -\nabla \times \widetilde{\boldsymbol{E}}, \tag{82c}$$

$$\partial_t \widetilde{H} = H, \tag{82d}$$

$$\partial_t H + \varepsilon_0^{-1}(\sigma_x + \sigma_y) H + \varepsilon_0^{-2} \sigma_x \sigma_y \widetilde{H} = \partial_t H^* + f, \tag{82e}$$

with exact solutions given as follows:

$$\begin{aligned}
&\boldsymbol{E} = \begin{pmatrix} E_x \\ E_y \end{pmatrix} = \begin{pmatrix} e^{-\pi t} \cos(\pi x) \sin(\pi y) \\ -e^{-\pi t} \sin(\pi x) \cos(\pi y) \end{pmatrix}, \quad \widetilde{\boldsymbol{E}} = \begin{pmatrix} (1 - \frac{\sigma_x}{\varepsilon_0 \pi}) E_x \\ (1 - \frac{\sigma_y}{\varepsilon_0 \pi}) E_y \end{pmatrix},\\
&H = e^{-\pi t} \cos(\pi x) \cos(\pi y), \quad \widetilde{H} = -\frac{1}{\pi} H, \quad H^* = -\frac{1}{\mu_0}(2 - \frac{\sigma_x + \sigma_y}{\varepsilon_0 \pi}) H.
\end{aligned}$$

While the corresponding source terms are given as

$$\begin{aligned}
&\boldsymbol{g} = \begin{pmatrix} g_x \\ g_y \end{pmatrix} = \begin{pmatrix} (-\pi \varepsilon_0 + \sigma_y + \pi)\, e^{-\pi t} \cos(\pi x) \sin(\pi y) \\ -(-\pi \varepsilon_0 + \sigma_x + \pi)\, e^{-\pi t} \sin(\pi x) \cos(\pi y) \end{pmatrix},\\
&f = e^{-\pi t} \cos(\pi x) \cos(\pi y) \left[(-\pi + \frac{\sigma_x + \sigma_y}{\varepsilon_0} - \frac{\sigma_x \sigma_y}{\pi \varepsilon_0^2}) - \frac{1}{\mu_0}(2\pi - \frac{\sigma_x + \sigma_y}{\varepsilon_0}) \right].
\end{aligned}$$

In this case, we have the following leapfrog type scheme: given initial approximations $\boldsymbol{E}_h^0, \widetilde{\boldsymbol{E}}_h^0, H_h^{\frac{1}{2}}, H_h^{*\frac{1}{2}}, \tilde{H}_h^{\frac{1}{2}}$, for any $n \geq 0$, find $\boldsymbol{E}_h^{n+1}, \widetilde{\boldsymbol{E}}_h^{n+1} \in \boldsymbol{U}_h^0$, $H_h^{n+\frac{3}{2}}, H_h^{*n+\frac{3}{2}}, \widetilde{H}_h^{n+\frac{3}{2}} \in \boldsymbol{V}_h$ such that

$$\begin{aligned}
\varepsilon_0 \left(\delta_\tau \boldsymbol{E}_h^{n+\frac{1}{2}}, \boldsymbol{\phi_h}\right) + \left(\Sigma^{**} \overline{\boldsymbol{E}}_h^{n+\frac{1}{2}}, \boldsymbol{\phi_h}\right) &= \left(H_h^{n+\frac{1}{2}}, \nabla \times \boldsymbol{\phi_h}\right)\\
&- \frac{\tau^2}{4\mu_0} \left(\nabla \times \delta_\tau \widetilde{\boldsymbol{E}}_h^{n+\frac{1}{2}}, \nabla \times \boldsymbol{\phi_h}\right) + \left(\boldsymbol{g}^{n+\frac{1}{2}}, \boldsymbol{\phi_h}\right), \quad \forall \boldsymbol{\phi_h} \in \boldsymbol{U}_h^0,
\end{aligned} \tag{83a}$$

$$\varepsilon_0 \left(\delta_\tau \widetilde{\boldsymbol{E}}_h^{n+\frac{1}{2}}, \widetilde{\boldsymbol{\phi}}_h\right) = \varepsilon_0 \left(\delta_\tau \boldsymbol{E}_h^{n+\frac{1}{2}}, \widetilde{\boldsymbol{\phi}}_h\right) + \left(\Sigma_{**} \overline{\boldsymbol{E}}_h^{n+\frac{1}{2}}, \widetilde{\boldsymbol{\phi}}_h\right), \quad \forall \widetilde{\boldsymbol{\phi}}_h \in \boldsymbol{U}_h^0, \tag{83b}$$

$$\mu_0 \left(\delta_\tau H_h^{*n+1}, \psi_h\right) = -\left(\nabla \times \widetilde{\boldsymbol{E}}_h^{n+1}, \psi_h\right), \quad \forall \psi_h \in \boldsymbol{V}_h, \tag{83c}$$

$$\left(\delta_\tau \widetilde{H}_h^{n+1}, \sigma_x \sigma_y \widetilde{\psi}_h\right) = \left(\overline{H}_h^{n+1}, \sigma_x \sigma_y \widetilde{\psi}_h\right), \quad \forall \widetilde{\psi}_h \in \boldsymbol{V}_h, \tag{83d}$$

$$\begin{aligned}
&\left(\delta_\tau H_h^{n+1}, \widehat{\psi}_h\right) + \varepsilon_0^{-1} \left((\sigma_x + \sigma_y) \overline{H}_h^{n+1}, \widehat{\psi}_h\right) + \varepsilon_0^{-2} \left(\sigma_x \sigma_y \widetilde{H}_h^{n+1}, \widehat{\psi}_h\right)\\
&\qquad = \left(\delta_\tau H_h^{*n+1}, \widehat{\psi}_h\right) + \left(f^{n+1}, \widehat{\psi}_h\right), \quad \forall \widehat{\psi}_h \in \boldsymbol{V}_h.
\end{aligned} \tag{83e}$$

We implement this scheme with different time step sizes $\tau = \frac{1}{2}h, \tau = h, \tau = 2h, \tau = 4h$ and varying mesh sizes h from $\frac{1}{24}$ to $\frac{1}{384}$. The obtained convergence rates of the L^2 errors at final time $T = 1$ are presented in Table 3, which shows that $\mathcal{O}(h)$ convergence can be obtained for both the electric field $\boldsymbol{E}$ and the magnetic field H without satisfying the CFL constraint.

Table 1: The L^2 errors obtained at $T = 1$ with $\tau = 4h, \tau = 2h, \tau = h, \tau = \frac{1}{2}h$ and various mesh sizes h.

h	$\tau = 4h$				$\tau = 2h$			
	$\\|\boldsymbol{E}-\boldsymbol{E}_h\\|$	Rate	$\\|H-H_h\\|$	Rate	$\\|\boldsymbol{E}-\boldsymbol{E}_h\\|$	Rate	$\\|H-H_h\\|$	Rate
$\frac{1}{24}$	1.7078E-03		1.8238E-03		1.2047E-03		1.0173E-03	
$\frac{1}{48}$	6.5253E-04	1.38800	6.1859E-04	1.55988	5.8366E-04	1.04554	4.8137E-04	1.07954
$\frac{1}{96}$	2.9831E-04	1.12923	2.5680E-04	1.26835	2.8946E-04	1.01175	2.3698E-04	1.02239
$\frac{1}{192}$	1.4555E-04	1.03534	1.2062E-04	1.09013	1.4443E-04	1.00297	1.1801E-04	1.00584
$\frac{1}{384}$	7.2318E-05	1.00904	5.9277E-05	1.02496	7.2179E-05	1.00075	5.8944E-05	1.00148
h	$\tau = h$				$\tau = \frac{1}{2}h$			
	$\\|\boldsymbol{E}-\boldsymbol{E}_h\\|$	Rate	$\\|H-H_h\\|$	Rate	$\\|\boldsymbol{E}-\boldsymbol{E}_h\\|$	Rate	$\\|H-H_h\\|$	Rate
$\frac{1}{24}$	1.1648E-03		9.4594E-04		1.1613E-03		9.4250E-04	
$\frac{1}{48}$	5.7869E-04	1.00919	4.7179E-04	1.00360	5.7826E-04	1.00599	4.7136E-04	0.99968
$\frac{1}{96}$	2.8884E-04	1.00251	2.3575E-04	1.00092	2.8879E-04	1.00171	2.3569E-04	0.99992
$\frac{1}{192}$	1.4436E-04	1.00065	1.1785E-04	1.00023	1.4435E-04	1.00045	1.1785E-04	0.99998
$\frac{1}{384}$	7.2169E-05	1.00017	5.8925E-05	1.00006	7.2169E-05	1.00012	5.8924E-05	0.99999

To test the time convergence rate, we solve this example again by fixing $\tau = \sqrt{h}$ and varying mesh sizes h from $\frac{1}{4}$ to $\frac{1}{256}$. The convergence rates of L^2 errors obtained at $T = 1$ are presented in Table 2, which justifies the theoretical convergence rate $O(\tau^2 + h)$ for the lowest order RTN spaces.

Table 2: The L^2 errors obtained at $T = 1$ with $\tau = \sqrt{h}$ and various mesh sizes h.

h	$\\|\boldsymbol{E}-\boldsymbol{E}_h\\|$	Rate	$\\|H-H_h\\|$	Rate
1/4	2.7006E-02		8.3175E-02	
1/16	3.4491E-03	1.48450	3.9255E-03	2.20259
1/64	8.0591E-04	1.04875	9.6349E-04	1.01327
1/256	1.9775E-04	1.01347	2.4668E-04	0.98281

Example 2. This example is used to test the long time stability of our scheme and the wave absorbing capability of this equivalent Bérenger's PML model. For this example, we choose the physical domain $\Omega = [0, 0.5]\,\mathrm{m}\times[0, 0.5]\,\mathrm{m}$, which is partitioned by a uniform triangular mesh with mesh size $h = 2.5 \times 10^{-3}\,\mathrm{m}$. We surround the physical domain by 20-layer PML cells with thickness $dd = 20h$. In our simulation, the damping

function σ_x is chosen as a fourth-order polynomial function given as:

$$\sigma_x(x) = \begin{cases} \sigma_{max}\left(\dfrac{x-0.5}{dd}\right)^4 & \text{if } x \geq 0.5, \\ \sigma_{max}\left(\dfrac{x}{dd}\right)^4 & \text{if } x \leq 0, \\ 0 & \text{otherwise,} \end{cases}$$

where $\sigma_{max} = -\log(err) * 5 * \varepsilon_0 * C_v/(2 * dd)$ with $err = 10^{-7}$ and C_v being the wave propagation speed in vacuum. The damping function σ_y has exactly the same form but in y variable.

This example is solved by the scheme (23a)-(23e) with zero initial fields and a point source wave located at $(0.25, 0.25)$, the center of the domain. The source wave is imposed on the H field given as $H = 0.1\sin(2\pi f t)$ with frequency $f = 3\,GH_z$.

Snapshots of the computed magnetic field H obtained with time step size $\tau = 2.5 \times 10^{-12}\,$s and up to 10000 time steps are plotted in Fig.1, which shows a long time stability of the scheme without obvious reflection from the surrounding PML cells.

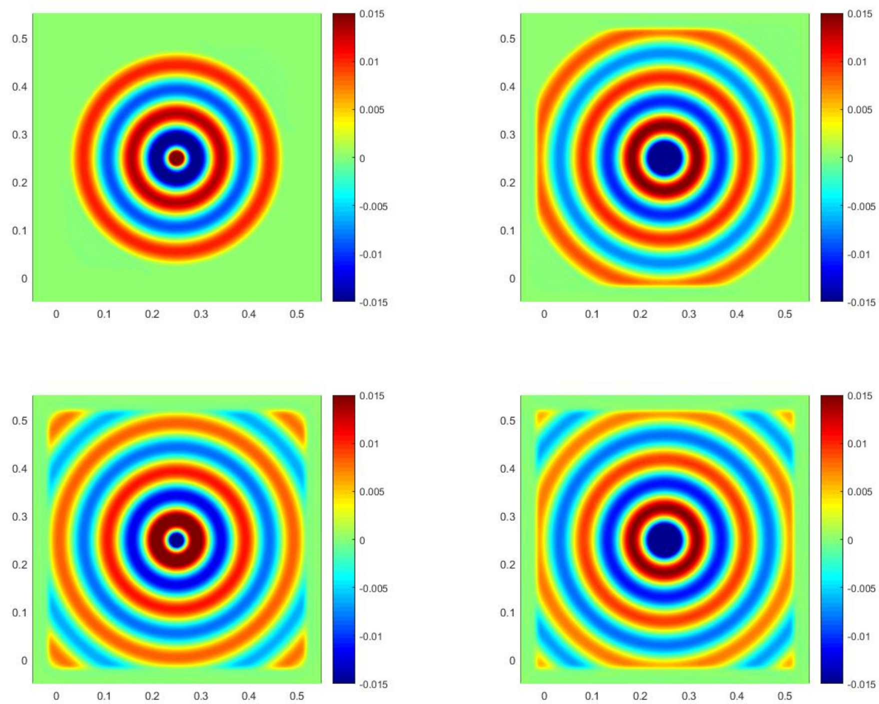

Figure 1: Magnetic field H at various time steps: (top left) 300 steps; (top right) 400 steps; (bottom left) 500 steps; (bottom right) 10000 steps.

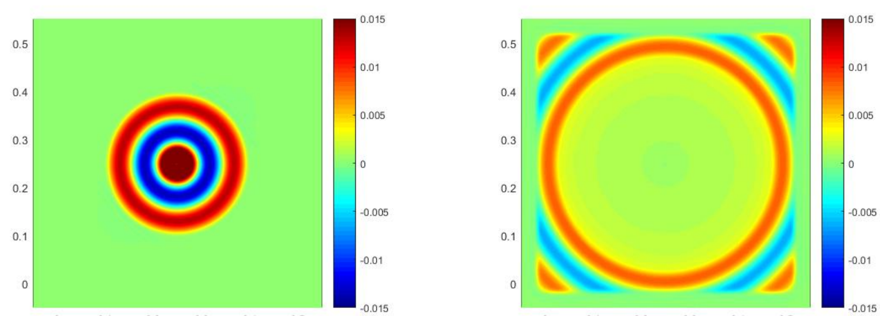

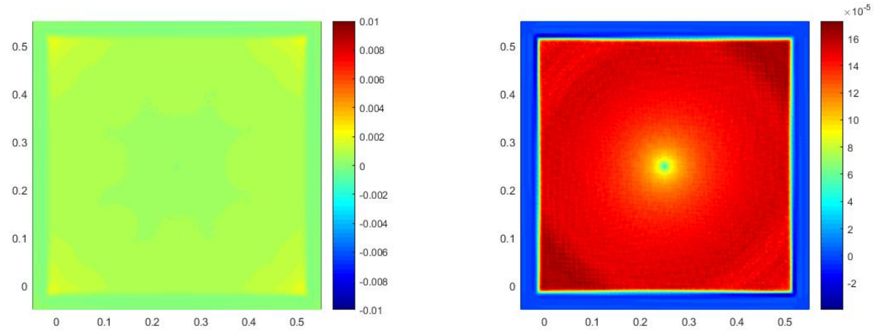

Figure 2: Snapshots of the magnetic field H: (top left) 200 steps; (top right) 500 steps; (bottom left) 700 steps; (bottom right) 1500 steps.

To see more clearly the performance of the PML model, we solve this example again by stopping the source wave after 200 time steps so that we can see how large the residual wave magnitude can be. Some snapshots of the magnetic fields H are plotted in Fig.2, which shows that the original source wave exits the domain without obvious reflections. The magnitude of the residual wave after 1500 time steps is about 2×10^{-4}, which is basically the numerical scheme error.

Example 3. This example is used to show the wave absorbing performance of our equivalent Bérenger's PML model with a line source wave. For this example, we choose $\Omega = [0, 2]\,\mathrm{m} \times [0, 2]\,\mathrm{m}$, which is surrounded by 8-layer PML cells with thickness $dd = 8h$. The incident source is imposed on the H field given as $H = \sin(2\pi f t)$ with frequency $f = 1.5\,GH_z$. To make a line source wave, the wave is placed on a line segment located at $x = 0.1\,\mathrm{m}$ with y ranging from $y = 0.5\,\mathrm{m}$ to $y = 1.5\,\mathrm{m}$. We use $h = 0.02\,\mathrm{m}$ and $\tau = 10^{-12}\,\mathrm{s}$ for this simulation.

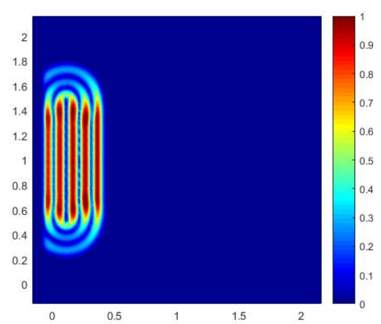

(a) $|H|$ at time step 1000

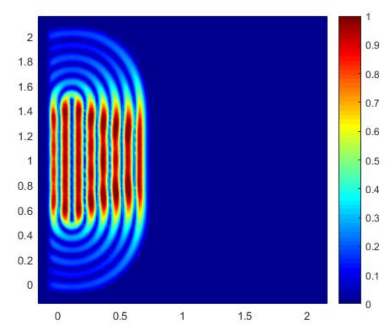

(b) $|H|$ at time step 2000

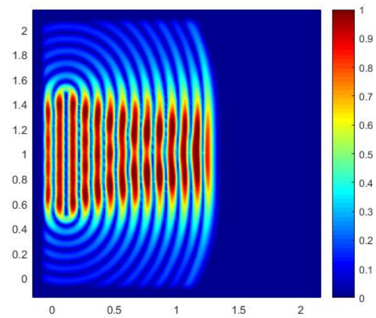

(c) $|H|$ at time step 4000

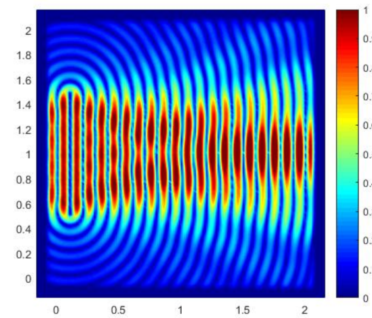

(d) $|H|$ at time step 8000

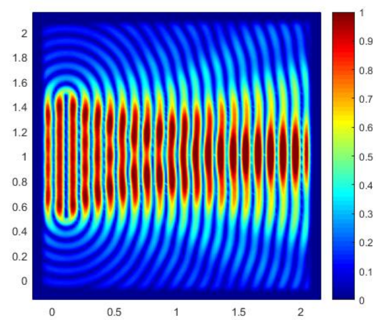

(e) $|H|$ at time step 15000

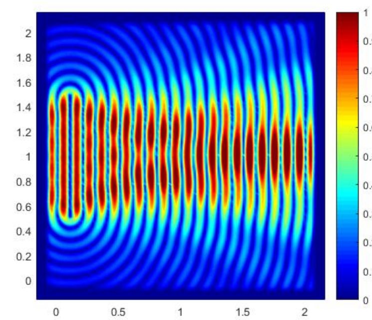

(f) $|H|$ at time step 20000

Figure 3: Snapshots of $|H|$ field obtained with $\tau = 10^{-12}\,$s at 1000, 2000, 4000, 8000, 15000, 20000 time steps.

Some snapshots of $|H|$ up to 20000 time steps are presented in Figure 3, which shows that out scheme enjoys a long stability and the wave propagates in the free space without obvious wave reflection from the truncated PML layers.

Example 4. This example is used to illustrate the dependence of the PML absorption capacity on the damping functions, especially on the PML thickness. By adopting a popular numerical strategy (e.g.,[34]), we impose the same source wave given as Example 2 at the center of the physical domain$\Omega_L = [0.125, 0.375]^2\,$m, which is discretized by a 100×100 cells. We surround the domain Ω_L by the equivalent Berenger's PML, whose damping functions and related parameters are the same as Example 2.

To measure the PML absorption performance, we solve the same problem in a very larger domain $\Omega_G = [-0.125, 0.625]^2\,$m, which is imposed by the PEC boundary condition and is discretized by a finite element mesh with the same mesh size in Ω_L. Then we calculate the errors of magnetic field H at element centers inside Ω_L by subtracting the corresponding solutions from those obtained on Ω_G. The global error energy is defined by the sum of the squares of those errors at element centers in Ω_L. To satisfy the CFL condition, we choose an initial time step $\tau_0 = 6.25 \times 10^{-13}\,$s and denote one time node (shortened as TN in Table 3) as 10 steps of τ_0, i.e. $1\,$time node $= 10\,\tau$. We carried out three experiments with PML thicknesses of dd=5h, 10h and 20h to observe the PML absorption capacity.

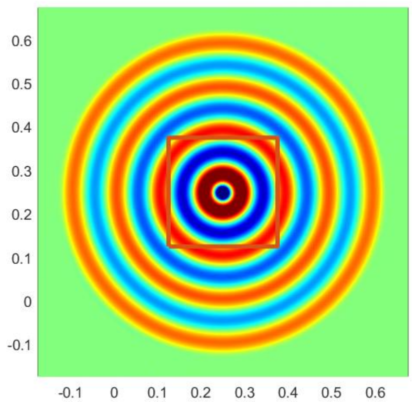

(a) Illustration of domains Ω_G and Ω_L.

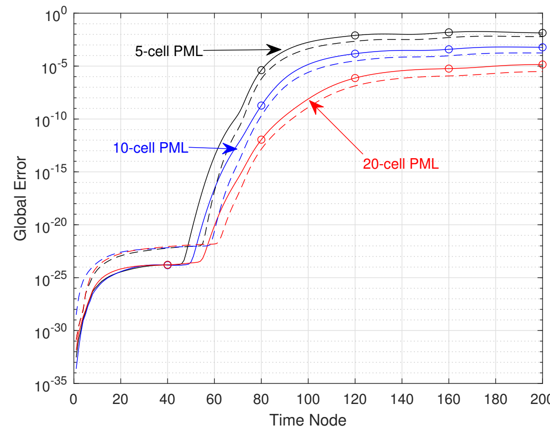

(b) The global errors obtained with three different PML thicknesses.

Figure 4: Example 4. The global errors obtained on a 100 $\times$ 100 mesh with a point wave source.

In Figure 4(a), the whole domain plotted is Ω_G, while the central squre suddomain marked by the red color is Ω_L. The Figure 4(b) compares the global errors versus time for the 5-cell, 10-cell, and 20-cell PMLs. As shown in Figure 4(b), the global reflection error is decreasing with the increasing of the PML's thickness, which is consistent with the common perfermance of PML [34]. For each fixed PML thickness, we tested two different mesh sizes: one with $h = 2.5 \times 10^{-3}$ m plotted by the solid line; and the other one with $h/2 = 1.25 \times 10^{-3}$ m plotted by the dashed line in Figure 4(b). Due to the dominance of the numerical error, we did not achieve the ideal reflection error 10^{-7} as chosen in σ_{max}. But we did observe the convergence rate $O(\tau^2 + h^2)$ in the discrete l^2 norm in Table 3. The $O(h^2)$ is a superconvergence phenomenon often happend for the lowest-order edge elements [22, Ch.5].

Table 3: The discrete l^2 errors for H_z of all points in Ω_L obtained with different layers PML at several time nodes.

TN	5-cell PML			10-cell PML			20-cell PML		
	h $\tau = \tau_0$	$h/2$ $\tau = \tau_0/2$	Rate	h $\tau = \tau_0$	$h/2$ $\tau = \tau_0/2$	Rate	h $\tau = \tau_0$	$h/2$ $\tau = \tau_0/2$	Rate
100	2.9873E-04	7.3744E-05	4.0509	2.6715E-05	5.6447E-06	4.7327	7.3547E-07	1.2557E-07	4.9777
105	3.8987E-04	9.9276E-05	3.9271	4.1648E-05	9.0136E-06	4.6205	1.3442E-06	2.7420E-07	4.9022
110	4.7247E-04	1.2282E-04	3.8469	5.7237E-05	1.2644E-05	4.5267	2.5325E-06	5.2451E-07	4.8283
115	5.5195E-04	1.4489E-04	3.8094	7.2170E-05	1.6214E-05	4.4511	4.1668E-06	8.7479E-07	4.7632
120	6.3073E-04	1.6659E-04	3.7862	8.6263E-05	1.9632E-05	4.3940	6.0986E-06	1.2955E-06	4.7077

5 Conclusion

In this paper, we developed a novel explicit unconditionally stable finite element scheme to solve an equivalent Bérenger's TEz PML model. We rigorously established both the stability and convergence analysis for the proposed scheme. Numerical results are presented to justify the theoretical analysis. We also demonstrated the effectiveness of this PML in simulating wave propagation in the free space. In the future, we will explore the possibility of extending similar idea to develop other explicit unconditionally stable schemes for other PML models [10].

Acknowledgments. The authors are very grateful to those two anonymous referees for their careful reading and insightful comments on improving our paper.

References

[1] S. Abarbanel, D. Gottlieb and J.S. Hesthaven, Non-linear PML equations for time dependent electromagnetics in three dimensions, J. Sci. Comput. 28 (2006) 125-137.

[2] D. Appelö, T. Hagstrom and G. Kreiss, Perfectly matched layers for hyperbolic systems: general formulation, well-posedness, and stability, SIAM J. Appl. Math. 67(1) (2006) 1-23.

[3] G. Bao, P. Li and H. Wu, An adaptive edge element method with perfectly matched absorbing layers for wave scattering by biperiodic structures, Math. Comp. 79 (2010) 1-34.

[4] E. Bécache and P. Joly, On the analysis of Bérenger's perfectly matched layers for maxwell's equations, ESAIM: M2AN 36 (2002) 87-119.

[5] E. Bécache, P. Joly, M. Kachanovska and V. Vinoles, Perfectly matched layers in negative index metamaterials and plasmas, ESAIM: Proceedings and Surveys 50 (2015) 113-132.

[6] E. Bécache and M. Kachanovska, Stable perfectly matched layers for a class of anisotropic dispersive models. Part I: necessary and sufficient conditions of stability, ESAIM: M2AN 51 (2017) 2399-2434.

[7] J.P. Bérenger, A perfectly matched layer for the absorbing EM waves, J. Comput. Phys. 114 (1994) 185-200.

[8] A.-S. Bonnet-Ben Dhia, L. Chesnel and P. Ciarlet, T-coercivity for scalar interface problems between dielectrics and metamaterials. ESAIM: M2AN 46 (2012) 1363-1387.

[9] J.H. Bramble and J.E. Pasciak, Analysis of a finite element PML approximation for the three dimensional time-harmonic Maxwell problem, Math. Comp. 77 (2008), no. 261, 1-10.

[10] M. Chen, Y. Huang and J. Li, Development and analysis of a new finite element method for the Cohen-Monk PML model, Numer. Math. 147 (2021) 127-155.

[11] G.C. Cohen and P. Monk, Mur-Nédélec finite element schemes for Maxwell's equations, Comput. Methods Appl. Mech. Eng. 169 (1999) 197-217.

[12] D. Correia and J.-M. Jin, 3D-FDTD-PML analysis of left-handed metamaterials, Microwave and Optical Technology Letters 40 (2004) 201-205.

[13] S.A. Cummer, Perfectly matched layer behavior in negative refractive index materials, IEEE Antennas and Wireless Propagation Letters 3(1) (2004) 172-175.

[14] K. Duru, L. Rannabauer, A.-A. Gabriel, G. Kreiss and M. Bader, A stable discontinuous Galerkin method for the perfectly matched layer for elastodynamics in first order form, Numer. Math. 146 (2020) 729-782.

[15] J.L. Hong, L.H. Ji and L.H. Kong, Energy-dissipation splitting finite-difference time- domain method for Maxwell equations with perfectly matched layers, J. Comput. Phys. 269 (2014) 201-214.

[16] Q. Hu, C. Liu, S. Shu and J. Zou, An effective preconditioner for a PML system for electromagnetic scattering problem, ESAIM: M2AN 49 (2015) 839-854.

[17] Y. Huang, M. Chen and J. Li, Development and analysis of both finite element and fourth-order in space finite difference methods for an equivalent Berenger's PML model, J. Comput. Phys. 405 (2020), 109154.

[18] Y. Huang, M. Chen and J. Li, Developing and analyzing new unconditionally stable leapfrog schemes for Maxwell's equations in complex media, J. Sci. Comput. 86 (2021), article 35.

[19] Y. Huang, H. Jia and J. Li, Analysis and application of an equivalent Berenger's PML model, J. Comp. Appl. Math. 333 (2018), 157-169.

[20] X. Jiang, P. Li, J. Lv and W. Zheng, An adaptive finite element PML method for the elastic wave scattering problem in periodic structures. ESAIM: M2AN 51 (2016) 2017-2047.

[21] J. Li and J.S. Hesthaven, Analysis and application of the nodal discontinuous Galerkin method for wave propagation in metamaterials, J. Comput. Phys. 258 (2014) 915-930.

[22] J. Li and Y. Huang, Time-Domain Finite Element Methods for Maxwell's Equations in Metamaterials, Springer Series in Computational Mathematics, vol.43, Springer, 2013.

[23] J. Li, C. Shi and C.-W. Shu, Optimal non-dissipative discontinuous Galerkin methods for Maxwell's equations in Drude metamaterials, Comput. Math. Appl. 73 (2017) 1768-1780.

[24] J. Li, C.-W. Shu and W. Yang, Development and analysis of two new finite element schemes for a time-domain carpet cloak model. Adv. Comput. Math. 48 (2022) Article 24, 30pp.

[25] Y. Lin, K. Zhang and J. Zou, Studies on some perfectly matched layers for one-dimensional time-dependent systems, Adv. Comput. Math. 30 (2009) 1-35.

[26] T. Lu, P. Zhang and W. Cai, Discontinuous Galerkin methods for dispersive and lossy Maxwell's equations and PML boundary conditions, J. Comput. Phys. 200 (2004) 549-580.

[27] P. Monk, Finite Element Methods for Maxwell's Equations, Oxford University Press, 2003.

[28] J.-C. Nédélec, Mixed finite elements in $\mathcal{R}^3$, Numer. Math. 35(3) (1980) 315-341.

[29] P.A. Raviart and J.M. Thomas, "A mixed finite element method for 2nd order elliptic problems", in "Mathematical aspects of the finite element method" (eds. by I. Galligani and E. Magenes). Lecture Notes in Mathematics, Vol. 606. Berlin-Heidelberg-New York: Springer 1977, pp. 292-315.

[30] A. Taflove and S.C. Haguess, Computational Electrodynamics: The Finite-Difference Time-Domain Method, 3rd edn., Artech House, Norwood, 2005.

[31] F.L. Teixeira and W.C. Chew, Advances in the theory of perfectly matched layers, edited by W.C. Chew et al. In: Fast and Efficient Algorithms in Computational Electromagnetics. Artech House, Boston (2001) 283-346.

[32] C. Wei, J. Yang and B. Zhang, Convergence of the uniaxial PML method for time-domain electromagnetic scattering problems, ESAIM: M2AN 55 (2021) 2421-2443.

[33] Z. Xie, J. Wang, B. Wang and C. Chen, Solving Maxwell's equation in meta-materials by a CG-DG method, Commun. Comput. Phys. 19 (2016) 1242-1264.

[34] L. Zhao and A.C. Cangellaris, A general approach for the development of unsplit-field time-domain implementations of perfectly matched layers for FDTD grid truncation, IEEE Microwave and Guided Wave Letters 6(5) (1996) 209-211.